info@fpinnovations.ca
www.fpinnovations.ca

Assessing the distribution of a local relative humidity dome created through large scale water cannon implementation

PROJECT NUMBER: 301014417

Brandon MacKinnon, M. Sc.

March 2022

Project number: 301014417

Technical report TR 2022 N23

ACKNOWLEDGEMENTS

This project was financially supported by Fire & Flood Emergency Services Ltd.

APPROVER CONTACT INFORMATION
Michael Benson
Manager, Wildfire Operations
Michael.Benson@fpinnovations.ca

REVIEWERS
Dave Schroeder, Alberta Wildfire

AUTHOR CONTACT INFORMATION
Brandon MacKinnon
Researcher, Wildfire Operations
Brandon.Mackinnon@fpinnovations.ca
(403) 312-1425

Table of contents

List of figures

List of tables

BACKGROUND

Relative humidity (RH) and temperature play a large role in the moisture content of available fuels, affecting the fire weather indices that indicate intensity, ignition, and spread potential of wildfires. However, the magnitude of increase in RH and decrease in temperature necessary to impact intensity and ignition potential is dependent on many additional factors including aspect, altitude, wind speed, atmospheric stability, fuel loading, fuel structure, and moisture content of the fuels.

The Canadian forest fire weather index (FWI) system is used to forecast fire behaviour in Canada as part of the Canadian forest fire behaviour prediction (FBP) system; the fine fuel moisture code (FFMC) is a key parameter taken into consideration when creating predictions for potential fire behaviour (Taylor et al., 1997). The FFMC represents the moisture content of litter and cured fine fuels; 1-2 cm in diameter. It expresses the relative ease of ignition and fine fuel flammability. The FFMC is sensitive to daily changes in temperature, rainfall, relative humidity, and wind speed. At a temperature of 20 °C and a relative humidity of 45%, the time lag is 2/3 of a day; this means that it takes ~16 hours for the fine fuels to lose 2/3 of the difference between its moisture content and its equilibrium moisture content at the new RH and dry bulb temperature. The rate at which fuel moisture responds to changes in RH and temperature is proportional to its diameter. Larger diameter fuels take exponentially longer to reach equilibrium than smaller fuels. However, extremely fine fuels such as dead grass, moss, and lichens respond have a lag time of only 1-4 hours. Furthermore, the equilibrium moisture content curves for absorption and desorption experience hysteresis, where the same RH on the absorption curve represents a lower fuel moisture content than on the desorption curve.

Scalable area-based high-volume water delivery systems have the ability to quickly move large amounts of water from one area to another. The pumps can deliver water through various sized hoses scalable to the desired outcome for distribution through water cannons to the landscape and the local environment. Furthermore, the direction, angle of spray, droplet size and distribution can be chosen by the operating technician to focus the water in one precise location or have it distributed to all 360 degrees.

Previous research completed by FPInnovations investigated the logistics and equivalent rainfall produced by the cannons investigated in this study (Refai & Hsieh, 2021). However, little is known about how much these systems influence the local atmospheric conditions on a large scale. To gain further knowledge on the topic, FPInnovations and Fire & Flood, a service provider of area-based high-volume water delivery solutions, collaborated to trial their 12-inch system. For the trial, 14 water cannons were spaced out on a harvested farm field ~9 km south west of Penhold, Alberta.

OBJECTIVE

Assess the vertical and horizontal distribution of RH and temperature surrounding a large-scale water cannon array.

METHODS

Water cannon layout

Setup of the water cannons started the day prior to testing and finished the following morning before the test commenced. Summaries of setup time and procedures can be found in previous assessments completed by FPInnovations regarding their 12-inch hose system and cannons (Refai and Hsieh, 2021); however the setup is more elaborate and took longer to setup.

Fourteen water cannons were setup in a previously harvested farmer's field (Figure 1) and the layout was chosen by Fire & Flood. The cannon layout was split up into an east and west suppression line, each with 7 cannons. The distance travelled by the supply line from the water source to the first cannon in each suppression line was approximately 1.6 km with an elevation gain of 37 m. The east and west suppression lines were each approximately 1.1 km long with an approximate elevation gain of 10 m (Figure 2). The area within immediate casting distance of the cannons will be referred to as the inundation zone. Distances of the data loggers to the inundation zone in metric and imperial can be found in Table 1.

Figure 1: Panorama of the inundation zone from the middle of the east side.

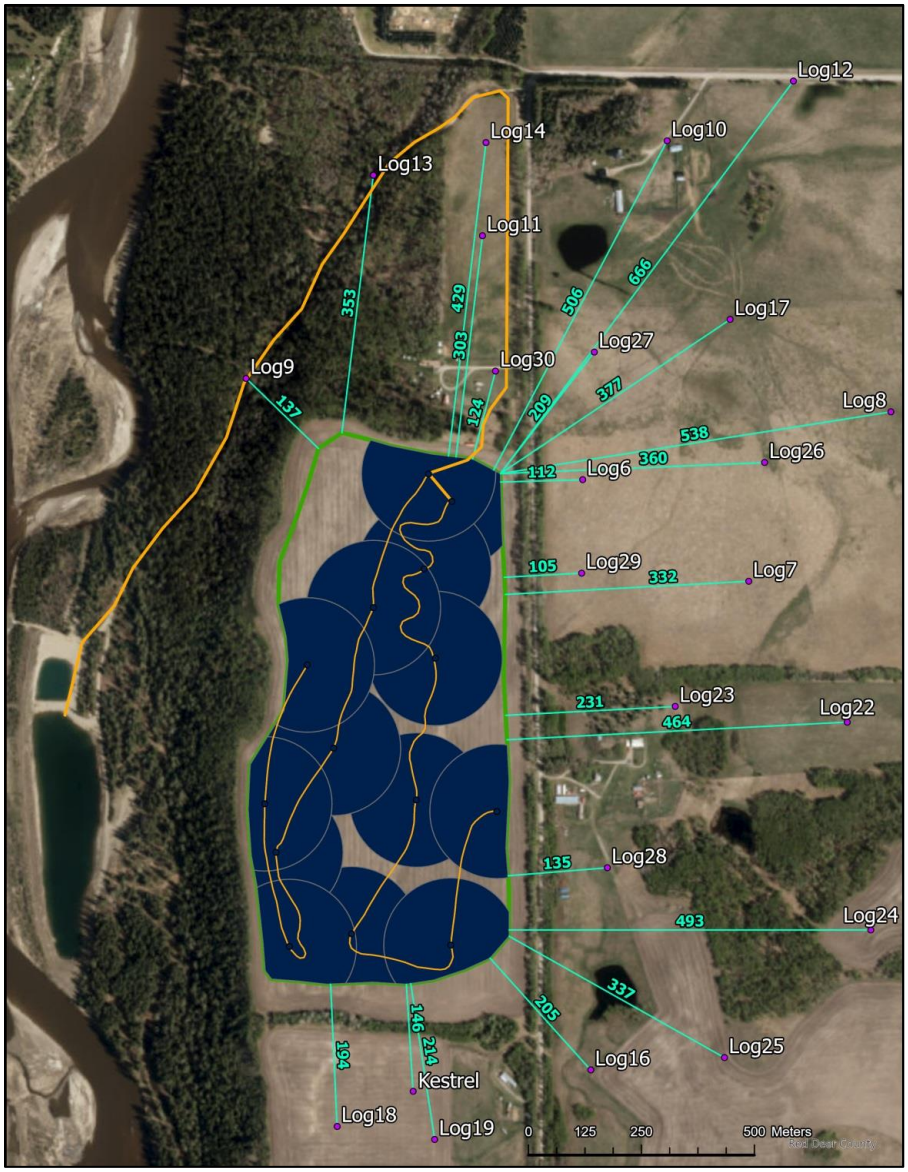

Figure 2: Site overview and ground data logger locations. Green numbers are distances in metres from the perimeter of the field to data logger locations. Yellow lines are the east and west control lines where the cannons are setup and the bold yellow is the supply line for the water cannons from the water source.

Table 1: Data logger locations and distance to inundation zone.

Point	Latitude	Longitude	Distance to inundation zone (m)	Distance to inundation zone (ft)
Kestrel	52.10263	-113.98283	146	481
Log06	52.1101	-113.97946	112	368
Log07	52.10886	-113.97616	332	1095
Log08	52.11093	-113.97333	538	1777
Log09	52.11134	-113.98615	137	453
Log10	52.11424	-113.97778	506	1670
Log11	52.11308	-113.98145	303	999
Log12	52.11497	-113.97527	666	2198
Log13	52.11382	-113.98362	353	1164
Log14	52.11422	-113.98138	429	1416
Log16	52.10289	-113.9793	205	675
Log17	52.112059	-113.976526	377	1243
Log18	52.1022	-113.98434	194	639
Log19	52.10204	-113.9824	214	708
Log22	52.10714	-113.9742	464	1531
Log23	52.10733	-113.97762	231	762
Log24	52.1046	-113.97373	493	1626
Log25	52.10304	-113.97664	337	1111
Log26	52.11031	-113.97584	360	1189
Log27	52.11166	-113.97923	209	689
Log28	52.10536	-113.97897	135	447
Log29	52.10896	-113.97948	105	347
Log30	52.11143	-113.98119	124	408

Ground relative humidity and temperature data logger layout

Ground data logger locations can be seen in Figure 2 (above). The data loggers were set to record data every 15 seconds and mounted on stakes at a height of approximately 45 cm above the ground surface (Figure 3). Reed R6020 temperature and RH data loggers were used on the ground and aerial platforms for consistency. 22 data loggers were set up for the experiment, but 2 data loggers were either damaged by cattle or failed to record quality data. As a result data loggers 17 and 27 were removed from the analysis. Specifications for the Reed R6020 were gathered from the manufacturer's website and can be seen in Table 2 below. It is important to acknowledge that the temperature readings may be marginally elevated and the RH values marginally decreased due to the absence of a fully aspirated Stevenson screen. However, the sensors are still ventilated and sheltered from direct solar insolation.

Figure 3: Reed R6020 ground setup

Table 2: Reed R6020 temperature and relative humidity data logger manufacturer specifications.

Temperature	
Measuring range	-40 to 158°F (-40 to 70°C)
Accuracy	±1.8°F (1.0°C)
Resolution	0.1°F/°C
Relative humidity	
Measuring range	0 to 100% RH
Accuracy	0 to 20% and 80 to 100%: ±5%
	20 to 40% and 60 to 80%: ±3.5%
	40 to 60%: ±3%
Resolution	0.1% RH

Weather station

The mobile weather station was a Kestrel 5500 located roughly 208-260m south of the nearest cannon locations (Figure 2). This was deemed a suitable location based off of the SpotWX forecast for the area that showed predominantly southwest winds during the testing period. This weather station served to gather baseline environmental weather conditions unaffected by the water distribution. The Kestrel weather station and data loggers 18 and 19 should remain unaffected by the cannons.

The Kestrel was attached to a camera tripod 1.5 m above the ground and the weathervane attachment was utilized (Figure 4). Recording interval was set to 30 seconds to capture any larger wind gusts during the testing period. Specifications for the Kestrel 5500 were gathered from the manufacturer's website and can be seen in Table 3 below.

Figure 4: Kestrel 5500 weather station setup.

Table 3: Kestrel 5500 manufacturer specifications.

Temperature	
Measuring range	-29 to 70°C
Accuracy	±0.5°C (1 m/s or greater wind reduces insolation effect)
Resolution	0.1°C
Relative humidity	
Measuring range	10-90% 25°C non-condensing
Accuracy	2% RH (direct sunlight may cause lower than actual RH values)
Resolution	0.1% RH
Wind	
Measuring range	2.2 to 144 km/h
Accuracy	Larger of 3% of reading, least significant digit or 20 ft/min speed
Resolution	0.1 km/h

Remotely piloted aircraft layout

DJI Matrice 210 and Matrice 300 remotely piloted aircraft systems (RPAS) were used to collect the aerial temperature and RH data. Four RPAS were used and stationed proximal to the cannons, to the north, to the east, and to the north-east (Figure 5). Data collection was focused on the downwind sections of the inundation zone due to the limited number of aircraft. Four Reed R6020 data loggers were tethered to each RPA and held at 25, 75, 125, and 175 feet above ground level (AGL) with the highest data logger tethered approximately 20 feet below the RPA.

Two 30-minute measuring periods were completed with stationary RPAs in different locations. The first measuring period was further away, as seen in Figure 5, and the second period was completed closer to the perimeter of the inundation zone. The RPA pilots attempted to keep the collection as continuous as possible, however they still needed to return periodically to their individual launch areas for battery changes (Figure 6).

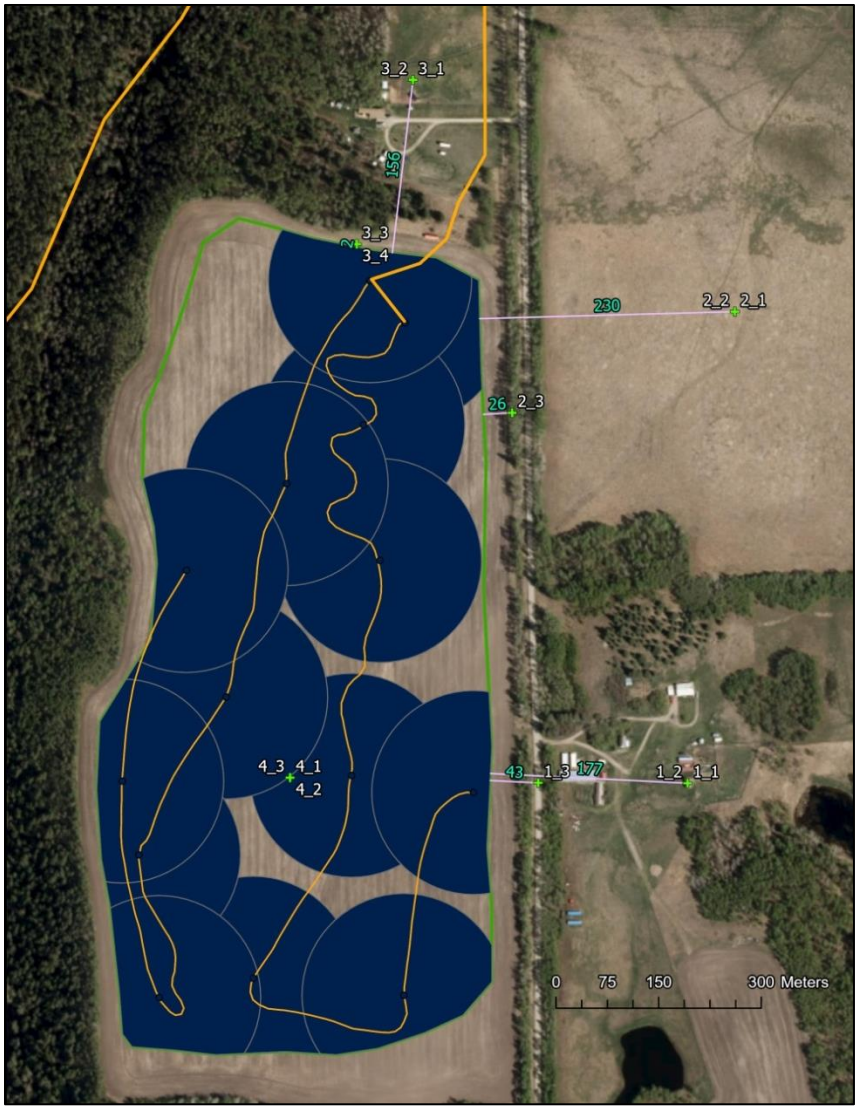

Figure 5: RPAS locations and distance from the perimeter of the water cannon inundation zone. Green values are distances in metres from the perimeter. The white writing near the "x" RPAS symbols designate the RPA number and flight respectively (2_2).

Figure 6: RPA performing a battery change during the testing period.

RESULTS

Weather

The morning of September 26 was fully cloud covered; however the afternoon was forecasted to be mainly sunny with clouds. As a result, the test was postponed until the temperature increased and the sun was visible. Once the sun came out the weather conditions were reflective of typical summer conditions. The test commenced at approximately 16:00 and finished at 17:30.

Wind

Wind recorded by the Kestrel 5500 was fairly consistent throughout the day with the larger gusts occurring earlier in the testing period. As the test progressed, the wind direction gradually transitioned from a primarily south-west direction to a west north-west direction upon termination of the testing. Wind throughout the day was primarily 8-18 km/h with gusts up to 24 km/h and quiet periods as seen in Figure 7. Surface values were multiplied by 1.5 to determine the 10m windspeeds.

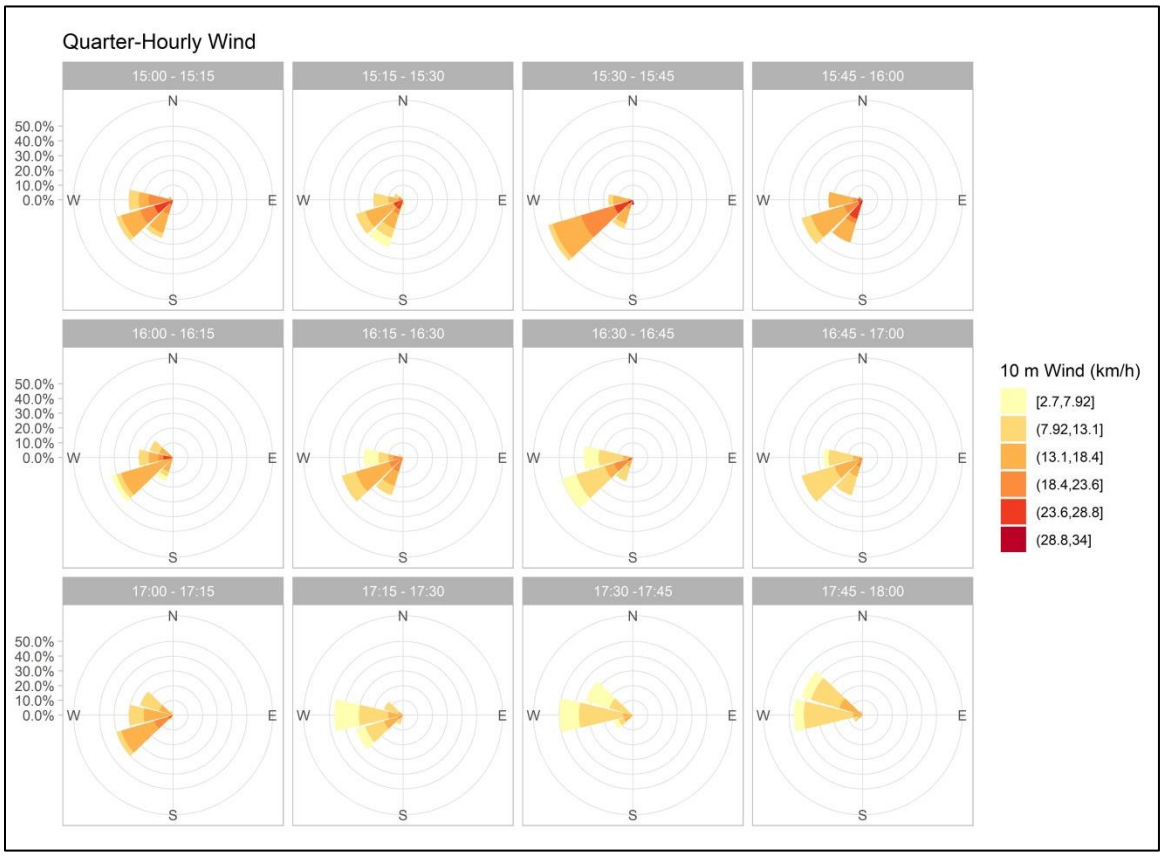

Figure 7: Kestrel 5500 wind rose data per quarter hour during the testing period.

Relative humidity and temperature

The values recorded by the kestrel were averaged over a ten minute time period so that the data represents a suitable time scale in a wildfire context. The averaged values help to reduce the spikes and troughs naturally found in the measurements that could be misleading upon initial investigation. Furthermore, the time interval for the averaging is still significantly shorter than the time lag for the smallest wildland fuels. In addition, this process was also implemented for the data recorded by the ground and aerial data loggers.

RH and temperature at the kestrel location (baseline) remained relatively constant throughout the day, with general trends of decreasing temperature and increasing RH. The high and low for temperature and RH respectively occurred around 15:30 (Figure 8). The RH and temperature were generally increasing (RH) and decreasing (temperature) throughout the test period and the rate of change increased after the test was terminated (17:30), likely due to the sun moving closer to the horizon. Sunset on September 26, 2022 occurred at 19:24.

The weather was representative of commonly occurring Alberta summer conditions with low RH and temperature close to “crossover”. Crossover occurs when the RH values fall below the temperature and it is a warning sign that extreme fire behaviour may be possible.

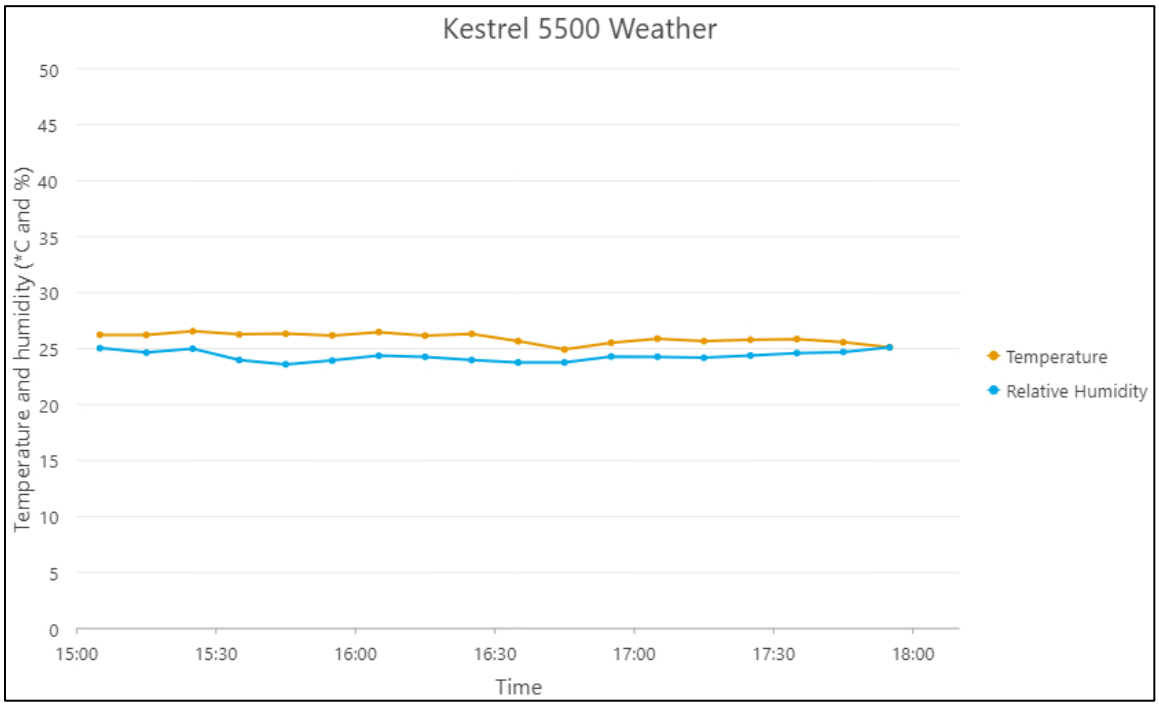

Figure 8: Kestrel 5500 temperature and RH during the testing period.

Ground relative humidity and temperature

Relative humidity

All data loggers experienced a drop in temperature and increase in relative humidity around 16:45, potentially indicating a change in cloud cover since the afternoon was mainly sunny though larger clouds were present. Cloud cover changes are the most likely cause, since the change occurred independently of any other measurable variables such as distance from the inundation zone or location relative to prevailing winds.

There is a variation in the starting conditions at each data logger. This variation can be influenced by microclimatic differences such as surface composition, insolation, and surrounding soil moisture. Therefore, focus should be weighted more towards trends within each data logger data set and the changes it experienced throughout the testing period.

The ground level RH increase averaged over all data loggers from the time the cannons were fully operational (16:20) till the termination of the test (17:30) was ~3.8%. This effect was more pronounced in the data loggers that were downwind of the cannons.

The average increase in RH for data loggers downwind of the cannons during the testing period (16:20 to 17:30) was 4.9% with a range of ~-1.4 to 12.2% (Appendix A: Table 4). Generally, the closer data loggers had a higher increase in RH. Data loggers 6, 28, 29, and 30 exhibited the highest ten minute average RH relative to pre-test values of approximately 11%, 27.8%, 5.4%, and 12.3% respectively during the test. The data loggers were located approximately 112, 135, 105, and 124m respectively from the perimeter of the inundation zone (Figures 9 and 2). However, the large jump in RH for data logger 29 near the end of the testing period also corresponds to a large temperature drop. This was an anomaly among the data loggers and it is likely that the data logger went into the shade around this time as the data logger was well within the path of the shade from the nearby trees when it was collected 30 minutes after the test was terminated.

Data loggers 13 and 9 consistently showed elevated RH values, however they were located in a valley to the north west of the test area and they were not downwind of the inundation zone. As a result, the readings do not seem to be influenced by the cannons since a linear trend can be seen before, during, and after the testing period (Figure 10). As these data loggers were outliers in the upwind dataset they were removed from the RH analysis for the ground data loggers. The upwind data loggers show a relatively stable RH profile with a modest increase of ~2.2% during the testing period (Appendix A: Table 5).

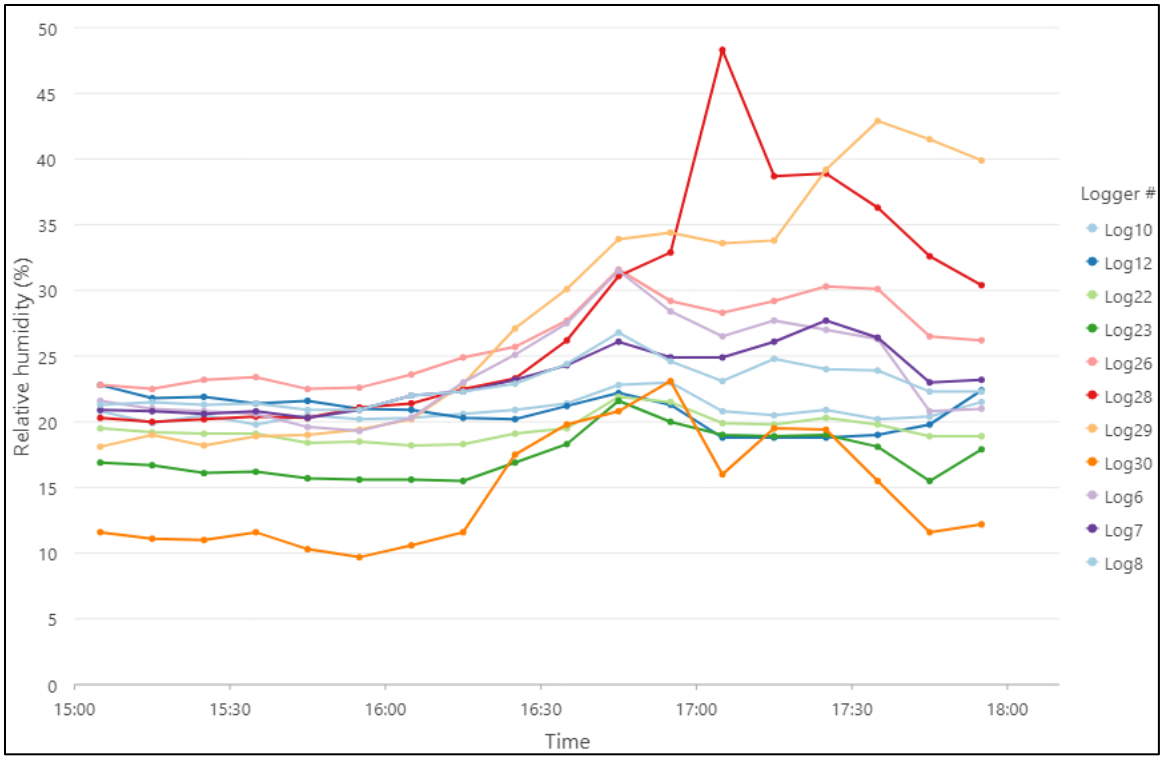

Figure 9: Downwind data logger relative humidity measurements.

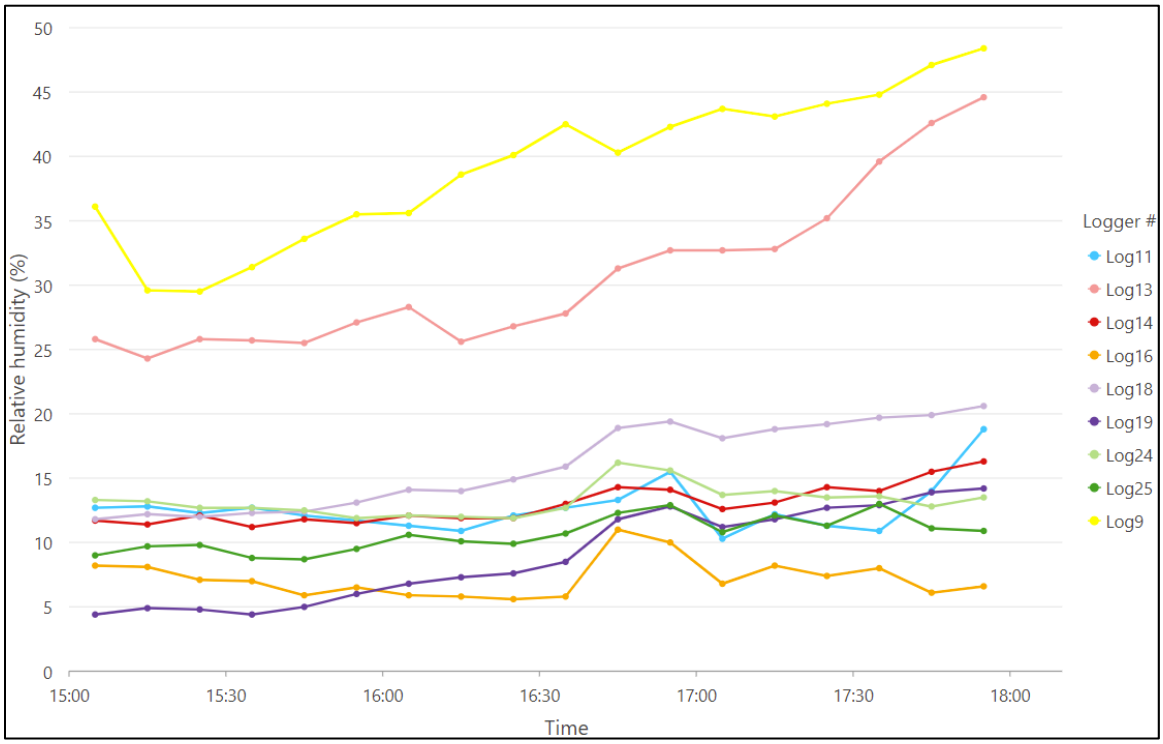

Figure 10: Upwind data logger relative humidity measurements.

Empirical Bayesian kriging is a geostatistical interpolation method for estimating data between known data points. The empirical Bayesian kriging results (Figure 11) show an estimated distribution of RH between the data loggers. The kriging values show good agreement with the information in the two figures (9 and 10) above. However, kriging is just an estimate and should only be used as a visual aid.

In summary, data loggers downwind and closer to the inundation zone experienced the largest increases in RH. Furthermore, when comparing Figures 7 and 11 for the time period used for the kriging, there is an association between wind direction and increased RH.

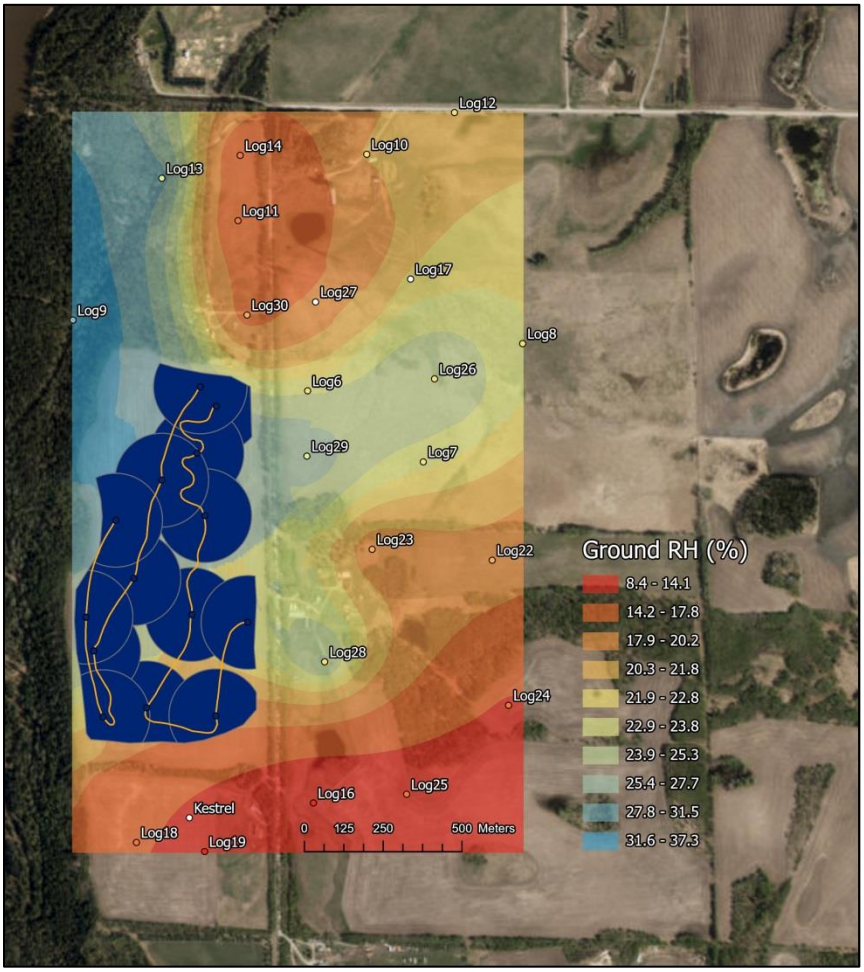

Figure 11: Ground level relative humidity interpolation using empirical Bayesian kriging at 16:30.

Temperature

Similar to the RH changes, all data loggers experienced decreases in temperature around 16:45 in agreement with the Kestrel weather station readings. The downwind and upwind temperature changes during the test period were within the accuracy of the R6020 data loggers and no significant differences were observed. There is a general trend of decreasing temperatures from the daytime high but this does not appear to be influenced by the presence of the cannons (Figures 12 and 13). Data loggers 9 and 13 indicate that the valley in the north-west has its own microclimatic differences compared to the other data logger locations. The temperatures of data loggers 6, 28, and 29 (Figure 12) do not seem to be influenced by the increases in RH noted above.

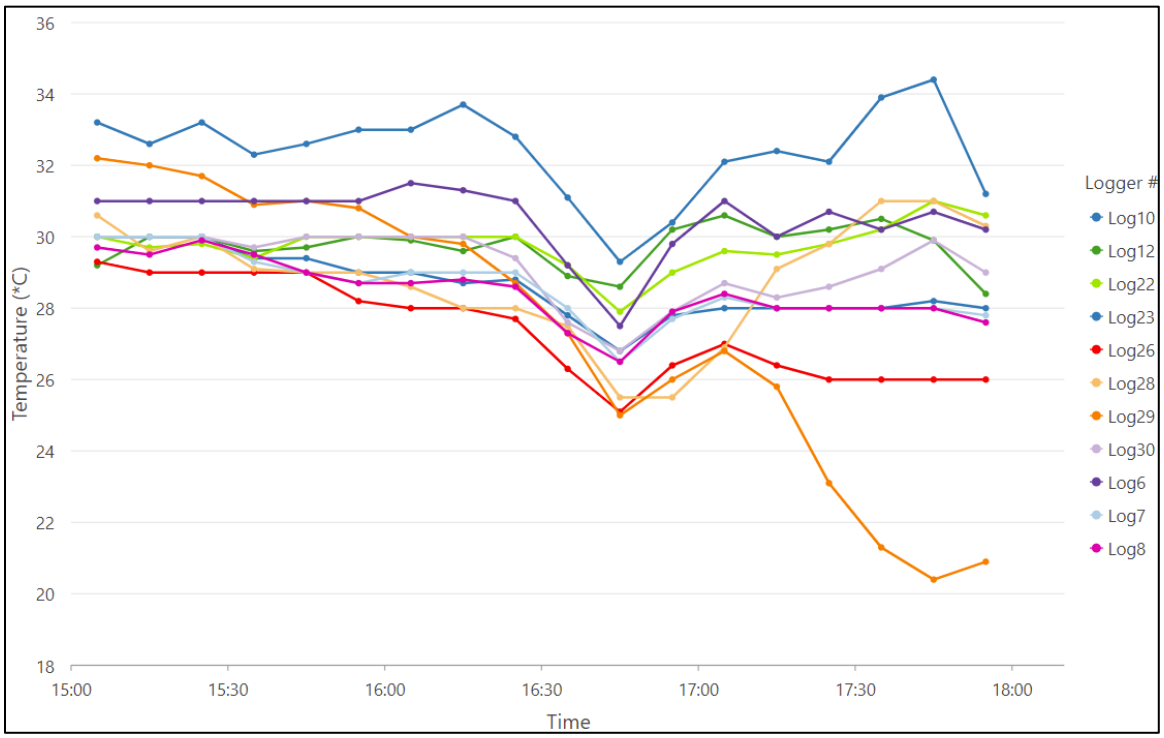

Figure 12: Downwind data logger temperature measurements.

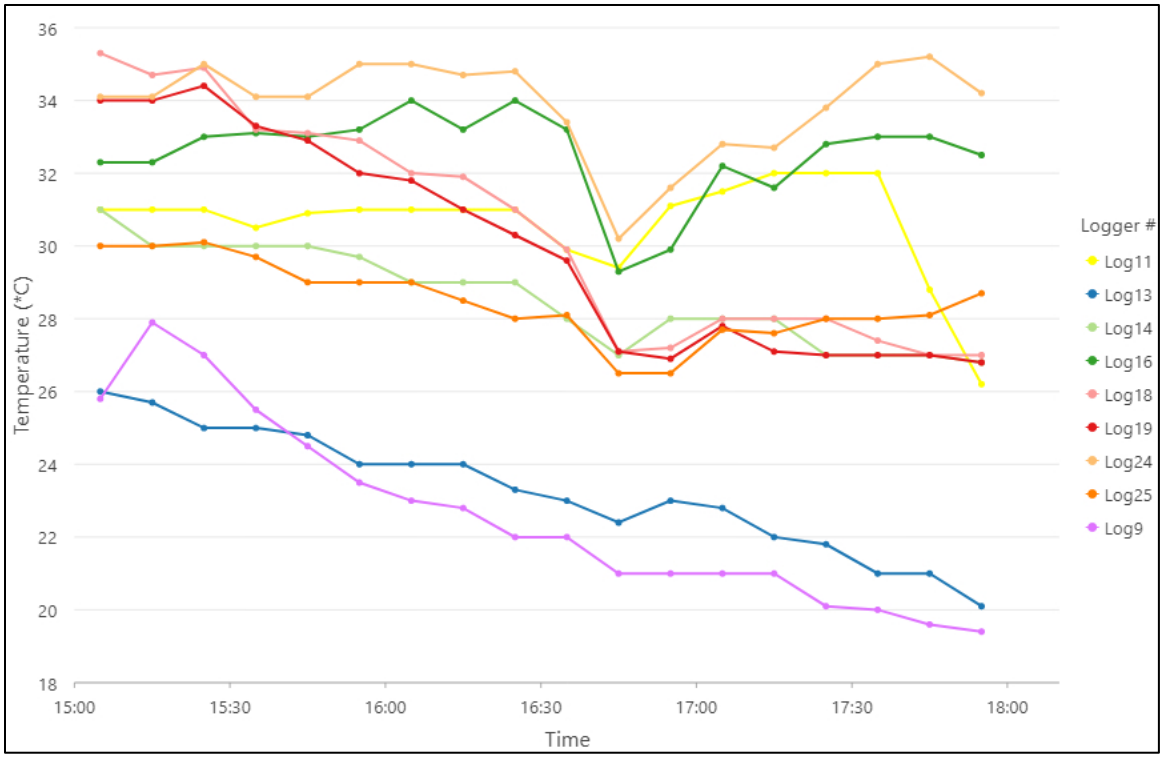

Figure 13: Upwind data logger temperature measurements.

The empirical Bayesian kriging shows strong influence from the two colder data loggers in the valley. However, the interpolation underestimates temperature in a few (data loggers 6, 10, 12, 22, 23, 30) of the downwind data loggers with an average underestimation of 1.1°C (Figure 14). The average standard error of the downwind data loggers is approximately -0.1°C. Furthermore, the interpolation standard error is inversely related to the data logger spatial density.

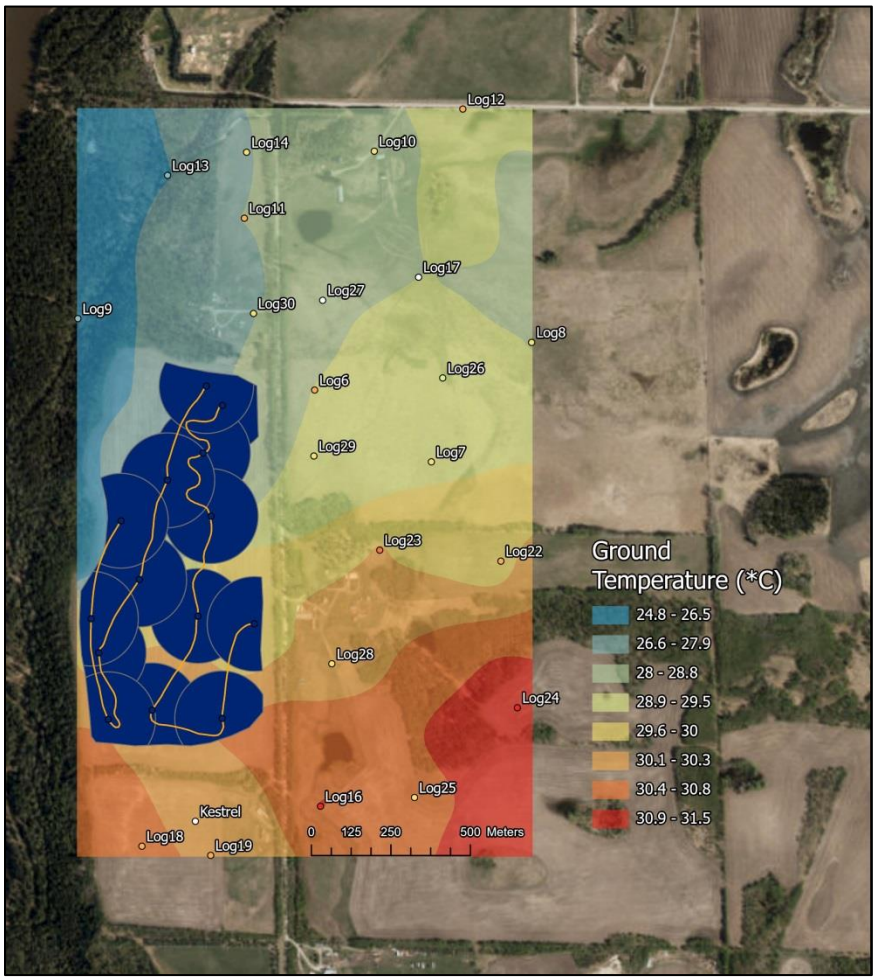

Figure 14: Ground level temperature interpolation using empirical Bayesian kriging at 16:30.

Aerial relative humidity and temperature

Relative humidity

Aerial RH increases were much larger than the ground level increases. The 25-ft above ground level (AGL) data loggers exhibited the highest increases in RH, some of them up to approximately 85% (Figure 15). The increase in RH at the 75, 125, and 175-ft AGL data loggers was not as pronounced as the 25-ft AGL data loggers, which measured increases in the RH of up to 65% from initial values. Increases in RH at 175-ft AGL seemed to be greater than those at 75 and 125-ft AGL. Flights close to the perimeter of the inundation zone (17:00 to 17:30) showed generally higher RH than the flights completed further away. The RH recorded by RPA 4, above the middle of the inundation zone was usually higher than all other locations. Empirical Bayesian kriging was not completed for each altitude since the four points would not provide enough data to interpolate with sufficient accuracy.

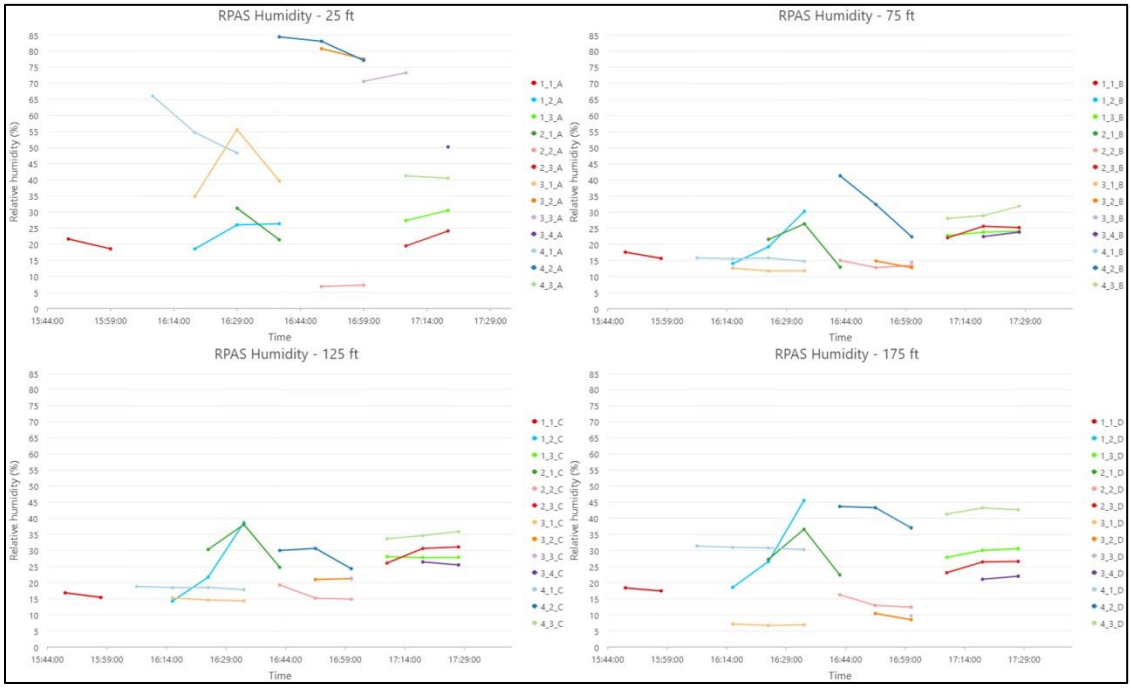

Figure 15: RPAS RH data. The labels for the figure correspond to the drone, flight number, and height (1_1_A). The letters A, B, C, and D correspond to altitudes of 25, 75, 125, and 175 ft AGL respectively. The drone and flight numbers can also be seen in Figure 5 in order to determine the location where the data was collected. The last flights between 17:00 and 17:30 were all completed closer to the perimeter of the field.

Temperature

Similar to the RH data, lower temperatures were observed in the 25-ft AGL data loggers, particularly in RPA 4 right above the inundation zone. Most of the other observable trends are within the error range of the data loggers and consist of only a 1-2°C variation in temperature. Decreases in temperature were not observed at other altitudes. The temperature variability between locations narrowed during the final portion of the test when the RPA's moved closer to the perimeter of the inundation zone; however, the temperatures were fairly similar (on average) to earlier flights.

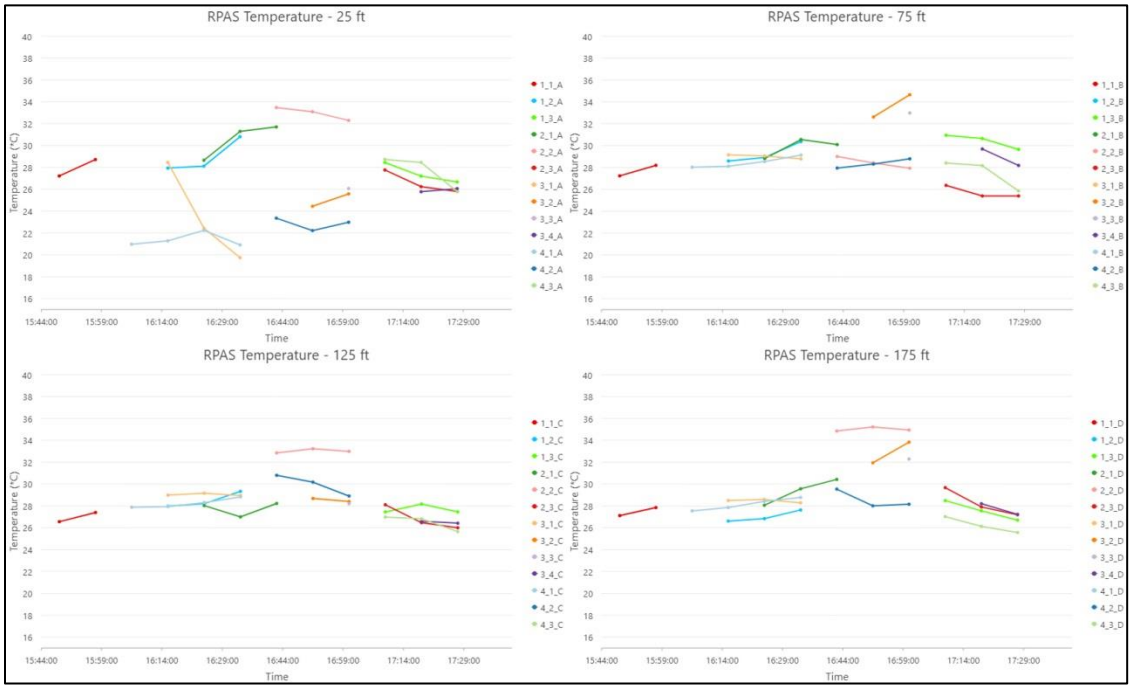

Figure 16: RPAS temperature data. The legends for each sub-figure correspond to the drone, flight number, and height (1_1_A). The letters A, B, C, and D correspond to altitudes of 25, 75, 125, and 175 ft AGL respectively. The drone and flight numbers can also be seen in Figure 5 in order to determine the location where the data was collected. The last flights between 17:00 and 17:30 were all completed closer to the perimeter of the field.

Water Cannons

The water cannons were turned on at approximately 15:50. Pressure increased and all cannons were functioning by 16:10, but were not yet at full operating pressure. At 16:15 some of the cannons were at full operating pressure but a few of them on the east control line were still operating at 50 psi. By 16:20 the cannons were fully functioning at ~110 psi and throughout the duration of the test maintained ~110-120 psi. When the cannons are operating at these pressures they are each dispersing approximately 3.6-4.0 m^3/min onto the landscape. Figures 17 and 18 show a view of the canons operating from the south east side of the inundation zone during the testing period.

Figure 17: View from the south showing the cannons functioning.

Figure 18: Cropped photo of the cannons operating from the south of the field, both control lines are visible.

CONCLUSIONS

Objective: Assess the vertical and horizontal distribution of RH and temperature surrounding a large-scale water cannon array.

The following conclusions can be drawn from the water cannon test:

1. Increases in RH at altitude were more pronounced than those at ground level
2. Increases in RH at 25 feet AGL were greater than the threshold to affect FFMC for dead fuels present at that height above the ground.
3. RH generally increased with decreasing altitude near the inundation zone.
4. Temperature at ground level remained relatively stable.
5. Increases in RH and decreases in temperature at altitude were most pronounced at the lowest altitude.
6. Increases in RH decreased with distance from the inundation zone, although detectable increases were recorded at data loggers distanced at 332 m (data logger 7 – 4%), 360 m (data logger 26 – 5.4%), and 538 m (data logger 8 – 2.8%) averaged over the testing period.
7. Increases in ground level RH were greatest within 135m downwind of the inundation zone.
8. Outside the inundation zone RH for some data loggers remained elevated but generally values returned to baseline within 15 minutes of pump shut off.
9. Ground level changes in RH and temperature are transient and dependent on the direction and magnitude of the wind.

It is unclear whether the differences in RH would have any measurable reduction in fire behaviour or ignition potential. Depending on the fuel type and other contributing factors, the increases in ground level RH within 150 m downwind of the inundation zone could potentially have a measurable impact on the fine fuel moisture code.

When consulting the diurnal Fine Fuel Moisture Code (FFMC) adjustment table in the Field Guide to the Canadian Forest Fire Behaviour Prediction (FBP) System (Taylor et al., 1997), during hypothetical high danger rating fire conditions (FFMC > 85) at 12:00, RH values of >52% would be required to reduce the standard daily FFMC. RH values of 35-54% at 11:00 would cause the standard daily FFMC to remain the same. Increases in RH values during the testing period would have been just enough to allow the standard daily FFMC within 135 m downwind of the inundation zone to remain static.

There may be increased benefit by running the cannons longer and earlier in the day. The diurnal adjustment table assumes a constant higher RH during the entire night and before the RH was measured that morning. This allows the fine fuels to reach equilibrium with the higher RH. To replicate the conditions surrounding the assumptions for the diurnal FFMC adjustment table, the water cannons would need to be running for periods of time similar to the equilibrium time lag for the fuels included in the FFMC. The equilibrium process can take several hours for the smallest size class fuels.

While the amount of water that can be transported and distributed by the system of interest onto the landscape is immense, the system in its assessed configuration and environmental conditions does not appear to provide lasting atmospheric increases in RH and decreases in temperature. Furthermore, the increases in RH during the test seem to be mostly experienced in the air above the inundation zone, close to the surface. Humid air, being less dense than dry air, tends to rise when surrounded by drier air; the test confirms this phenomenon. Finally, any data logger locations experiencing increases in ground level RH seem to be influenced primarily by prevailing winds.

BIBLIOGRAPHY

Refai, R. & Hsieh, R. (2021). Area-Based Water Delivery Systems: Exploratory research on logistics, water delivery, and its localized impacts. FPInnovations. URL: https://wildfire.fpinnovations.ca/Research/ProjectPage.aspx?ProjectNo=220.

Taylor, S. W., Pike, R. G., & Alexander, M. E. (1997). Field Guide to the Canadian forest fire behaviour prediction (FBP) system. Canadian Forest Service.

APPENDIX A: INDIVIDUAL GROUND RH FIGURES AND SUBSEQUENT ANALYSIS

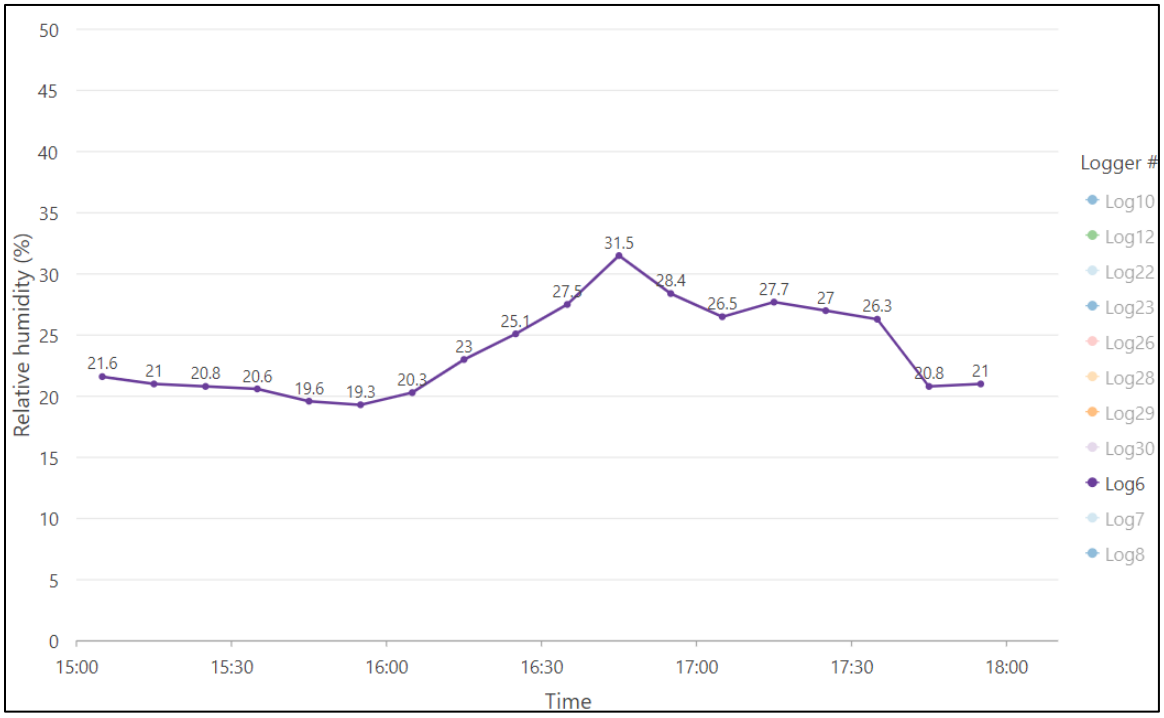

Figure 19: Downwind data logger 6 RH during the testing period using a 10 minute average of values.

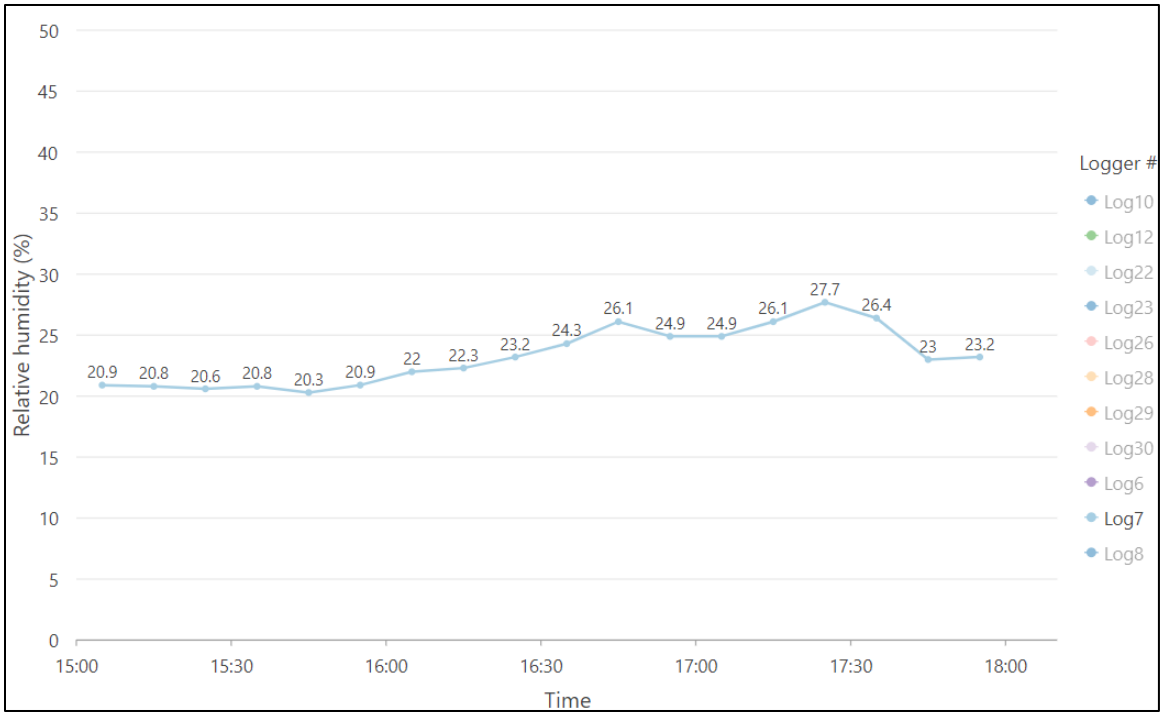

Figure 20: Downwind data logger 7 RH during the testing period using a 10 minute average of values.

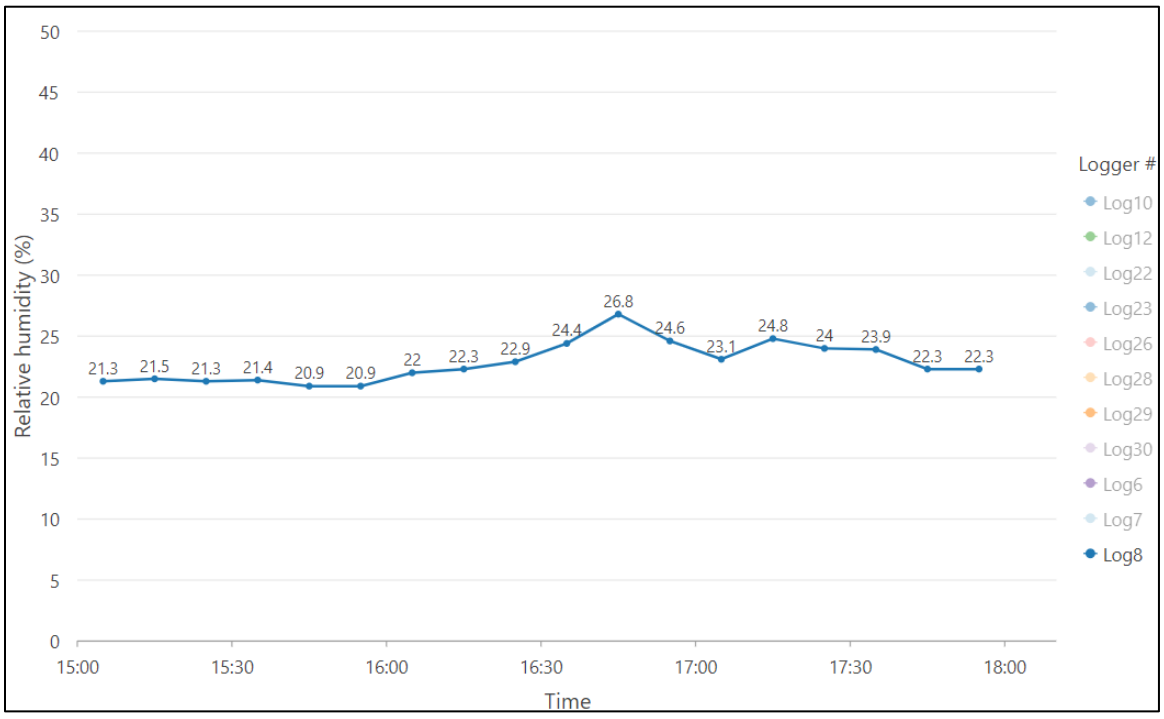

Figure 21: Downwind data logger 8 RH during the testing period using a 10 minute average of values.

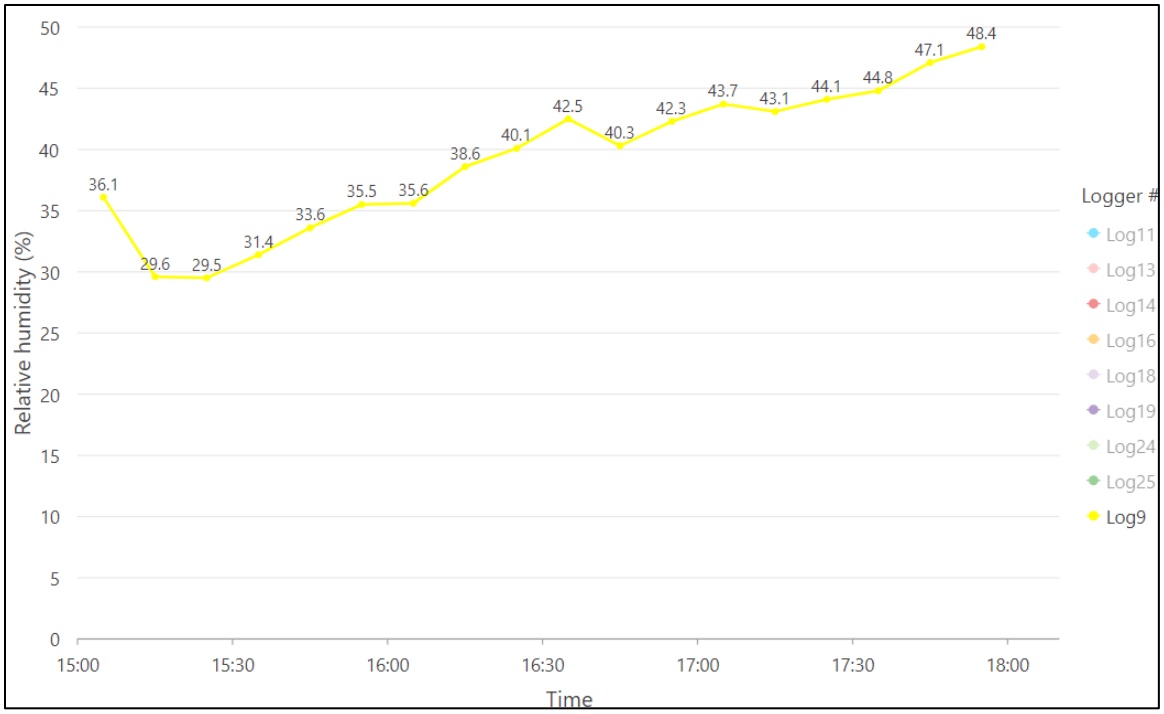

Figure 22: Upwind data logger 9 RH during the testing period using a 10 minute average of values.

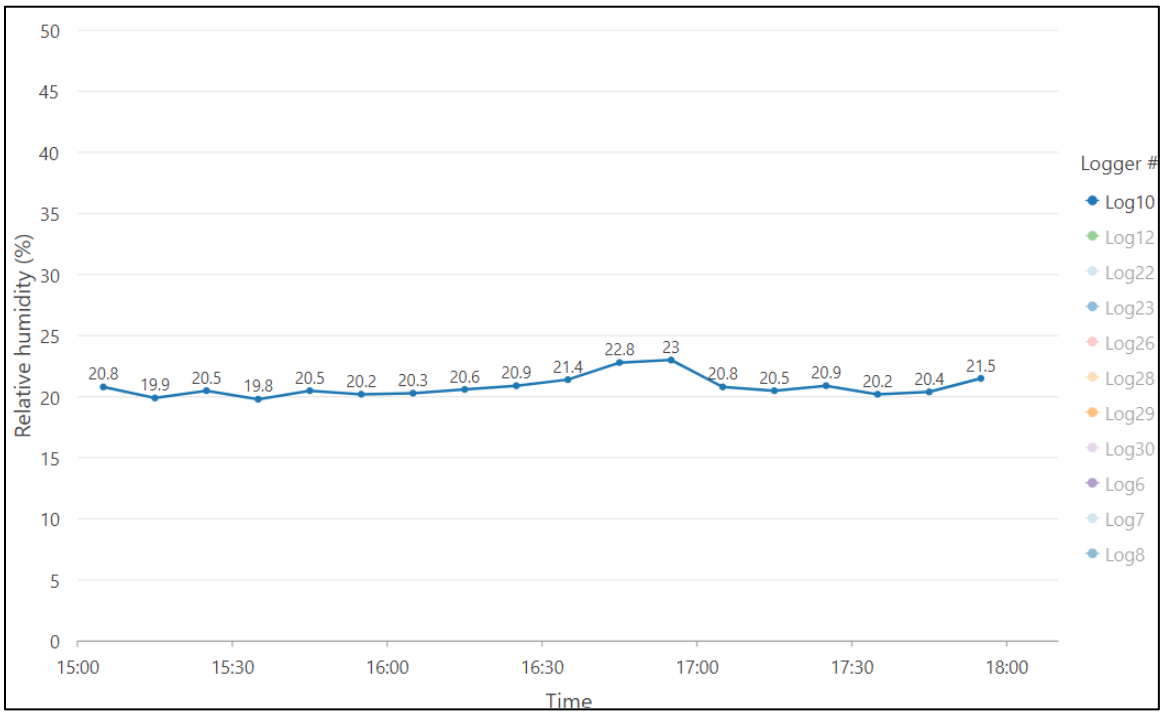

Figure 23: Downwind data logger 10 RH during the testing period using a 10 minute average of values.

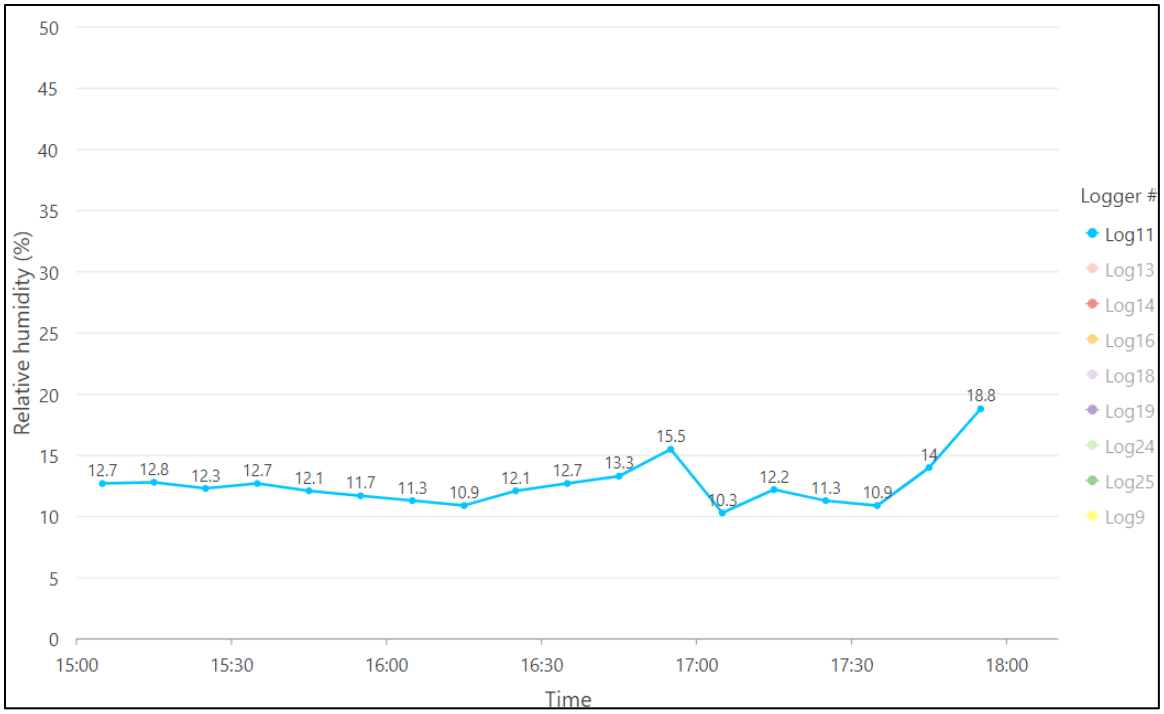

Figure 24: Upwind data logger 11 RH during the testing period using a 10 minute average of values.

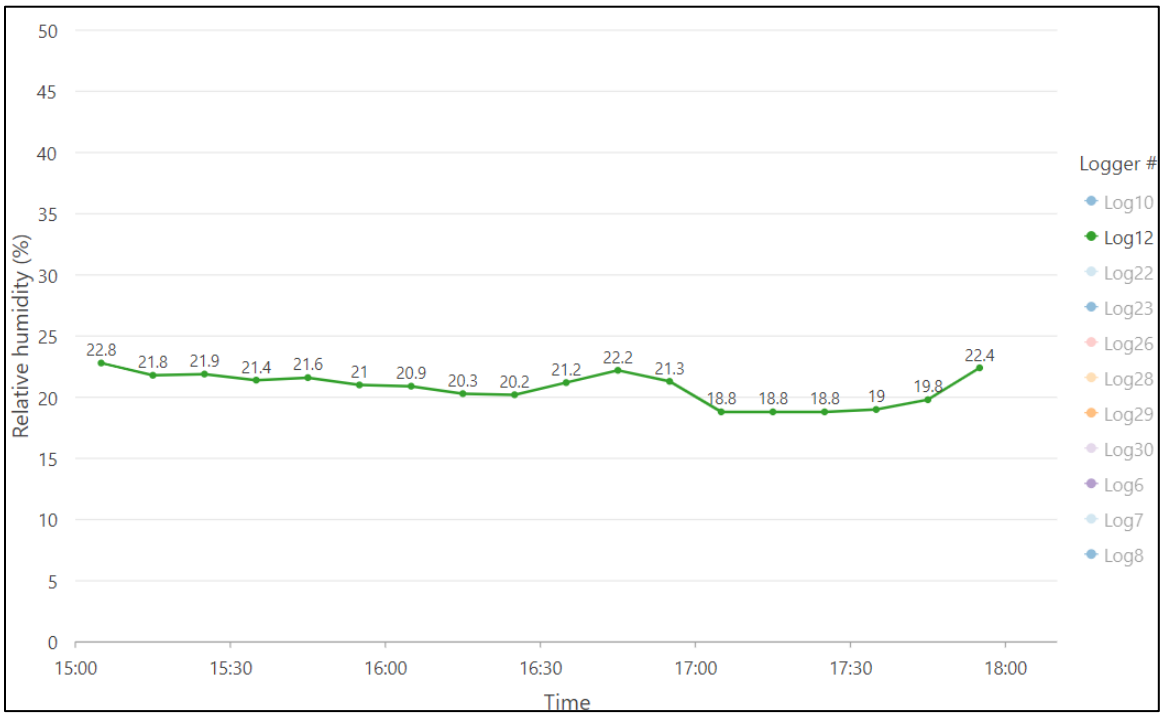

Figure 25: Downwind data logger 12 RH during the testing period using a 10 minute average of values.

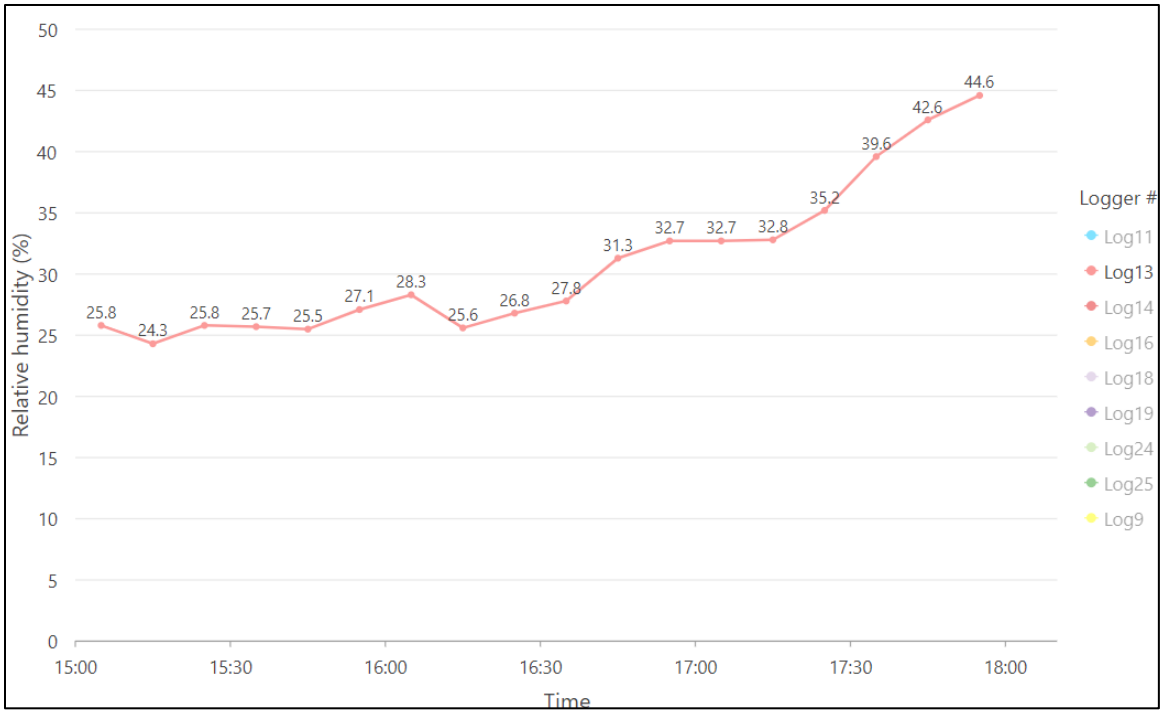

Figure 26: Upwind data logger 13 RH during the testing period using a 10 minute average of values.

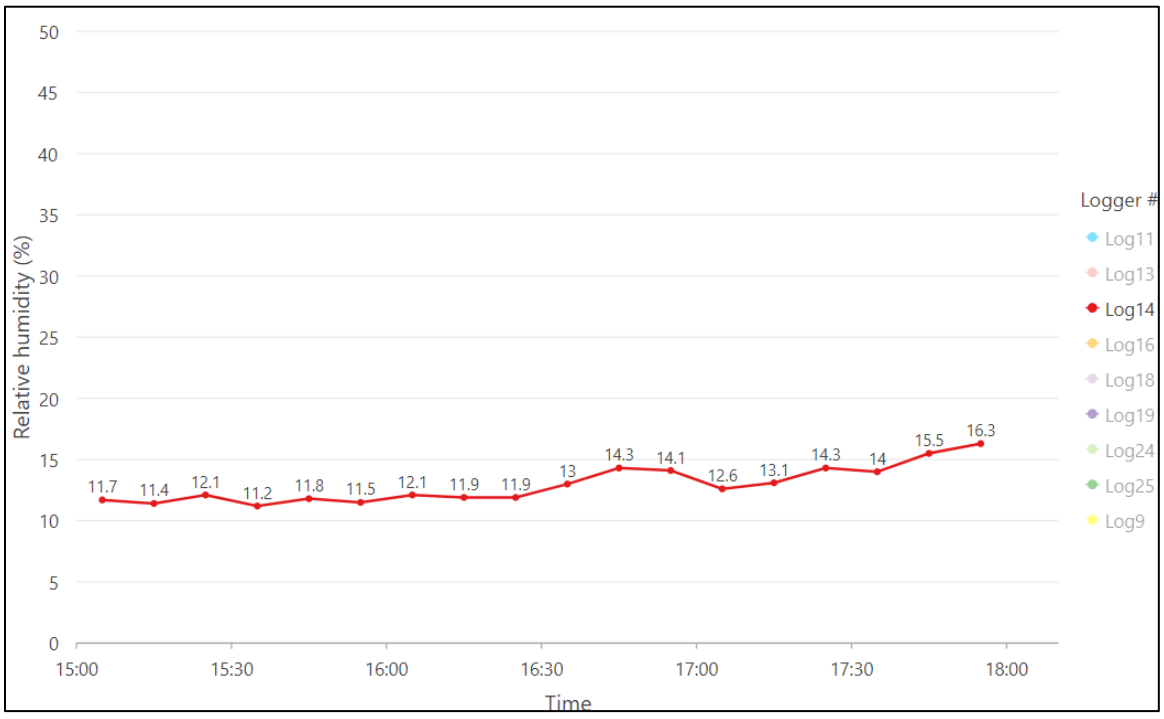

Figure 27: Upwind data logger 14 RH during the testing period using a 10 minute average of values.

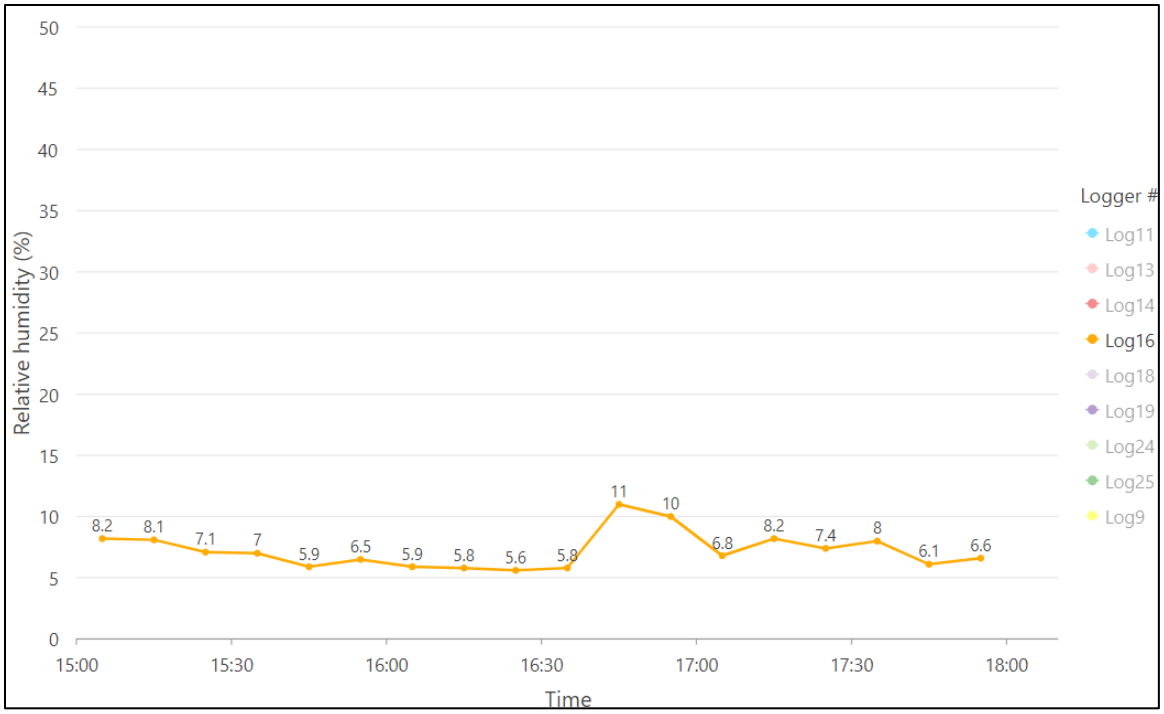

Figure 28: Upwind data logger 16 RH during the testing period using a 10 minute average of values.

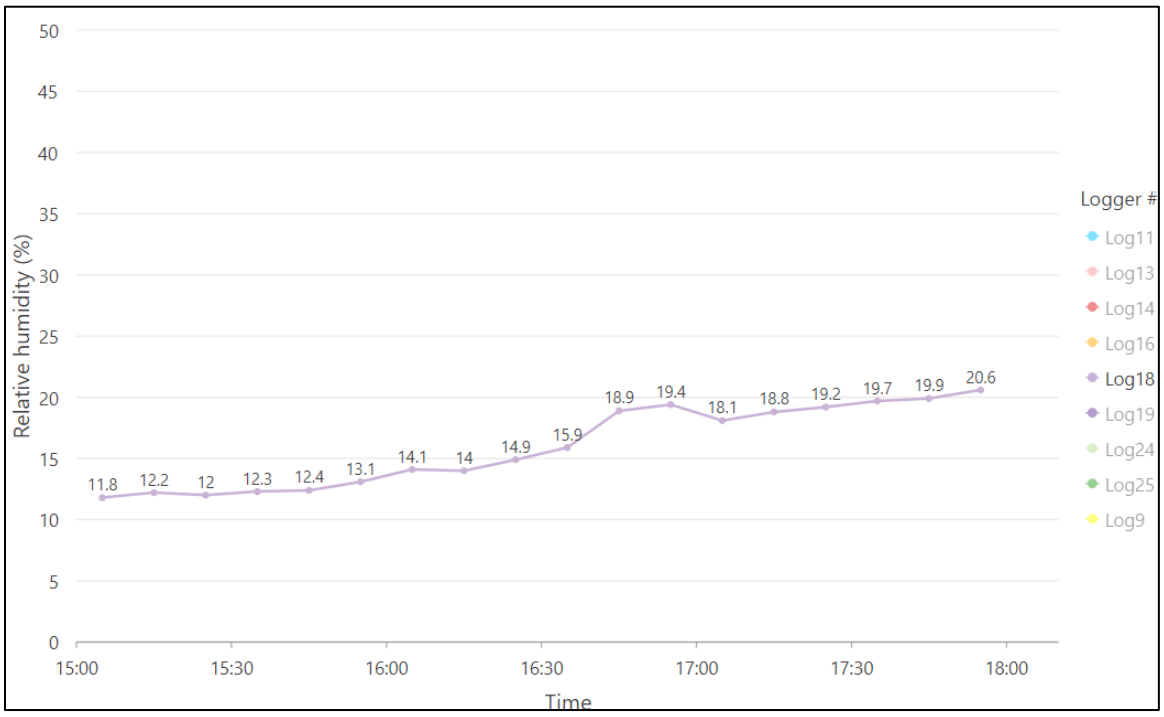

Figure 29: Upwind data logger 18 RH during the testing period using a 10 minute average of values.

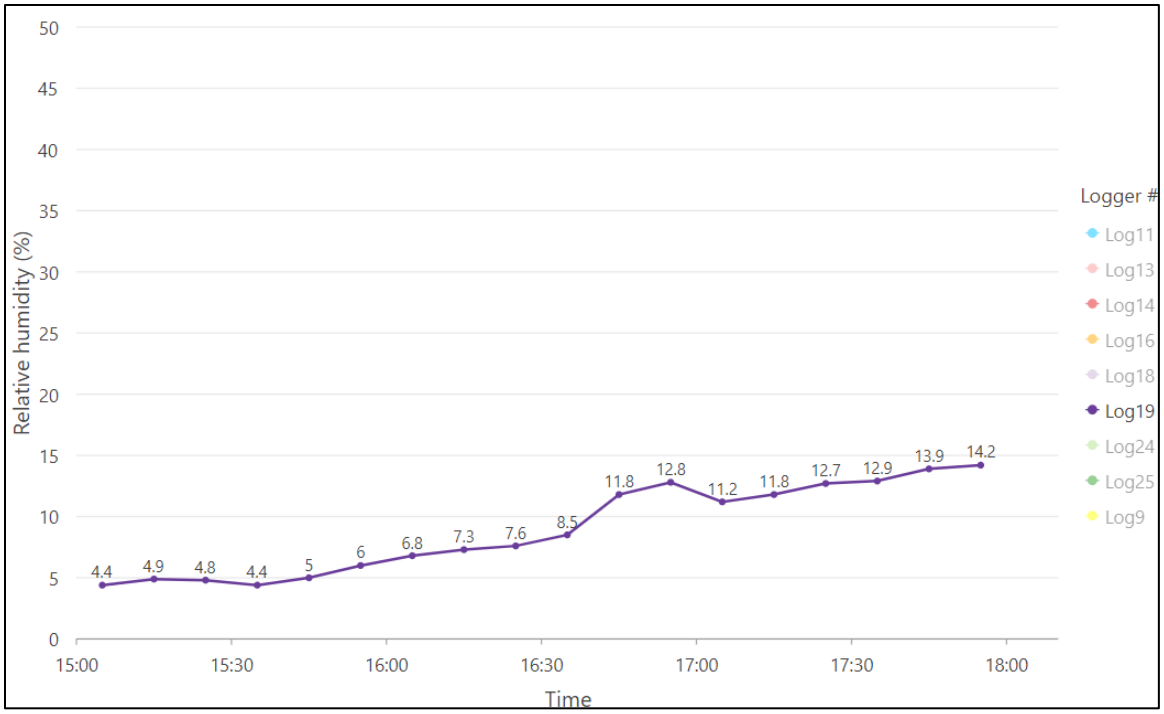

Figure 30: Upwind data logger 19 RH during the testing period using a 10 minute average of values.

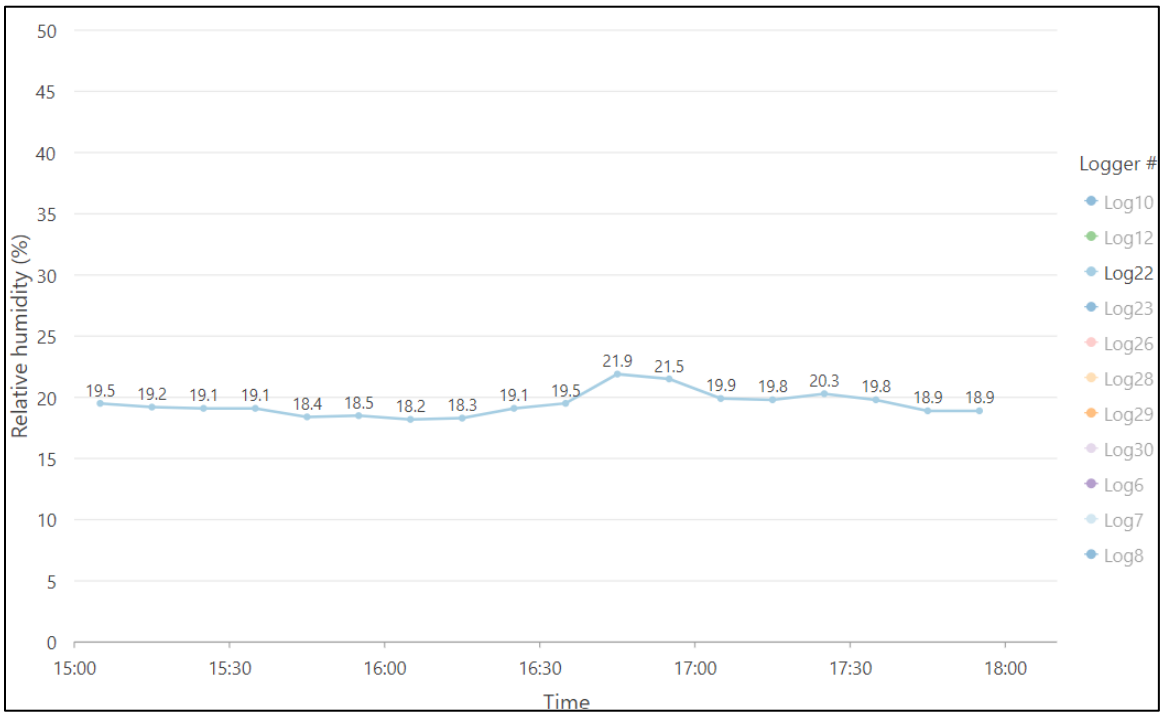

Figure 31: Downwind data logger 22 RH during the testing period using a 10 minute average of values.

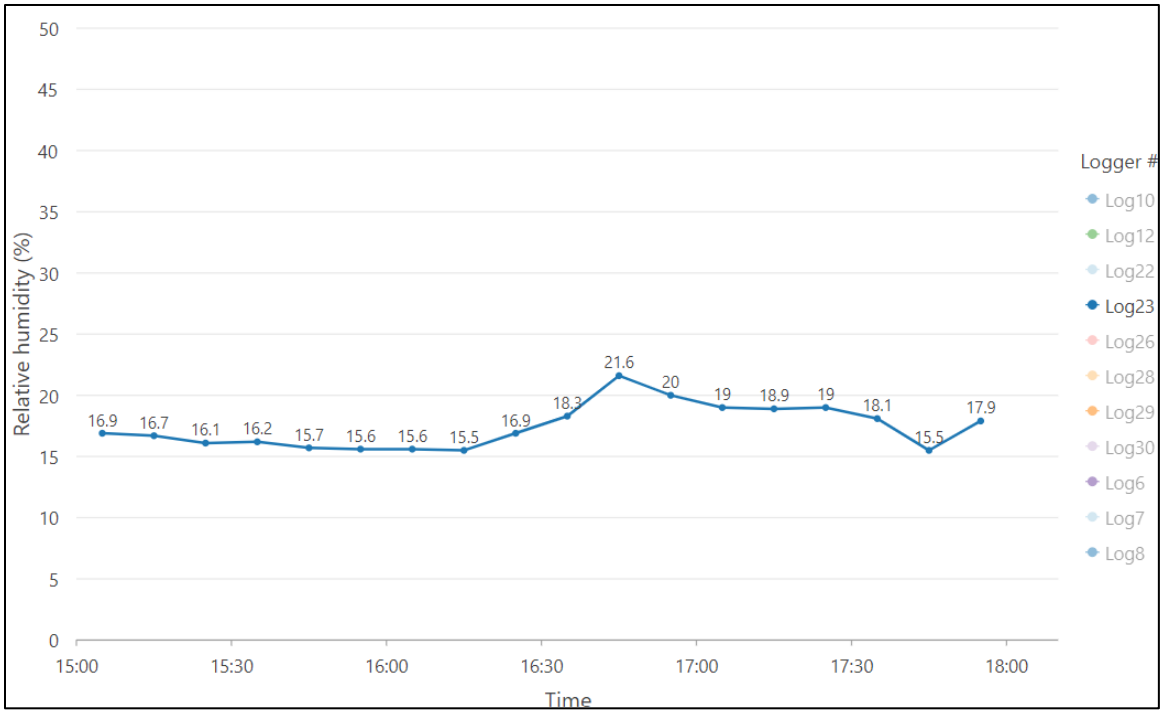

Figure 32: Downwind data logger 23 RH during the testing period using a 10 minute average of values.

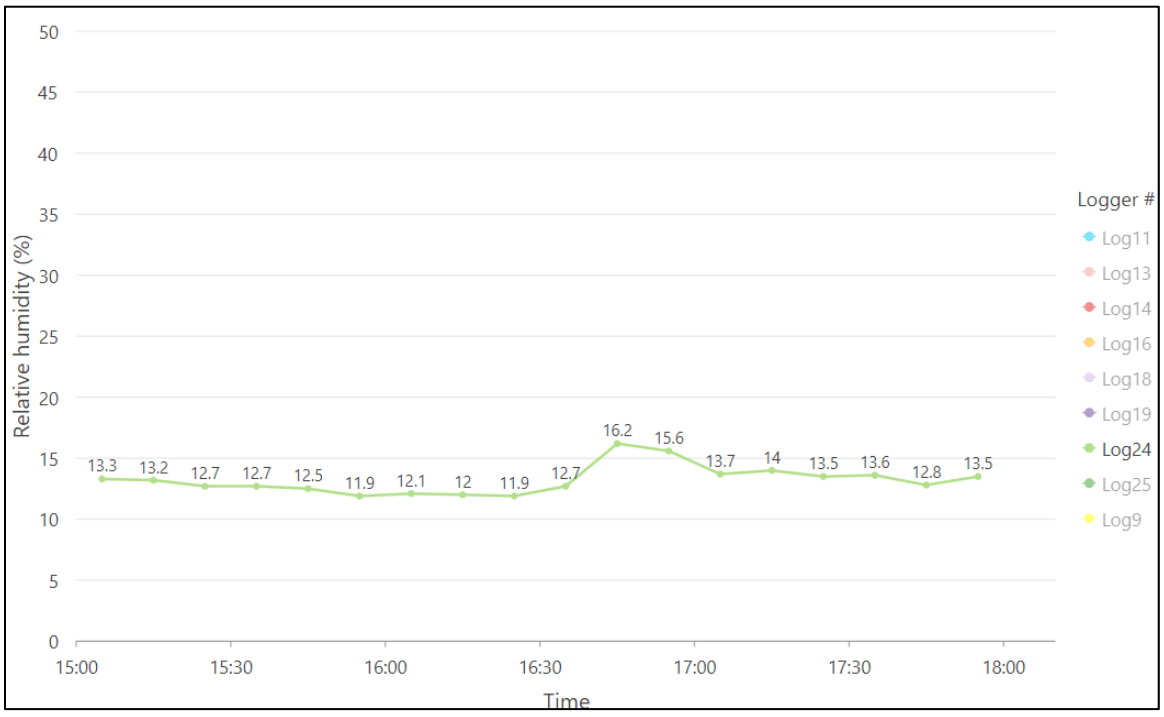

Figure 33: Upwind data logger 24 RH during the testing period using a 10 minute average of values.

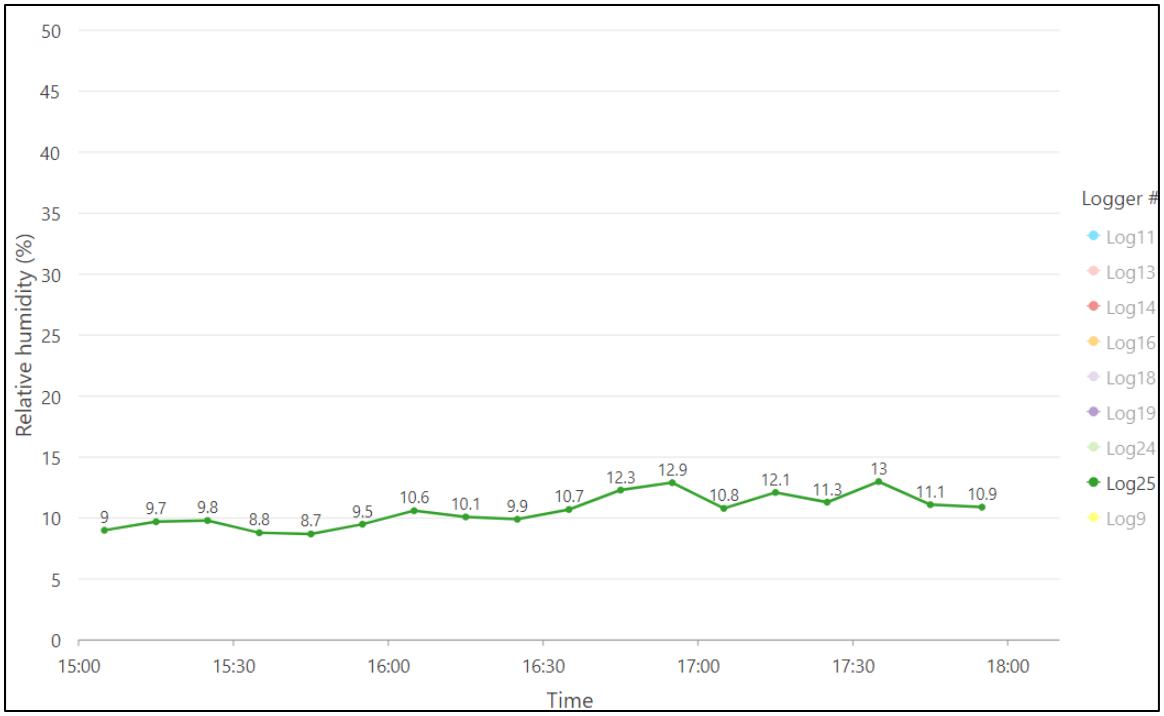

Figure 34: Upwind data logger 25 RH during the testing period using a 10 minute average of values.

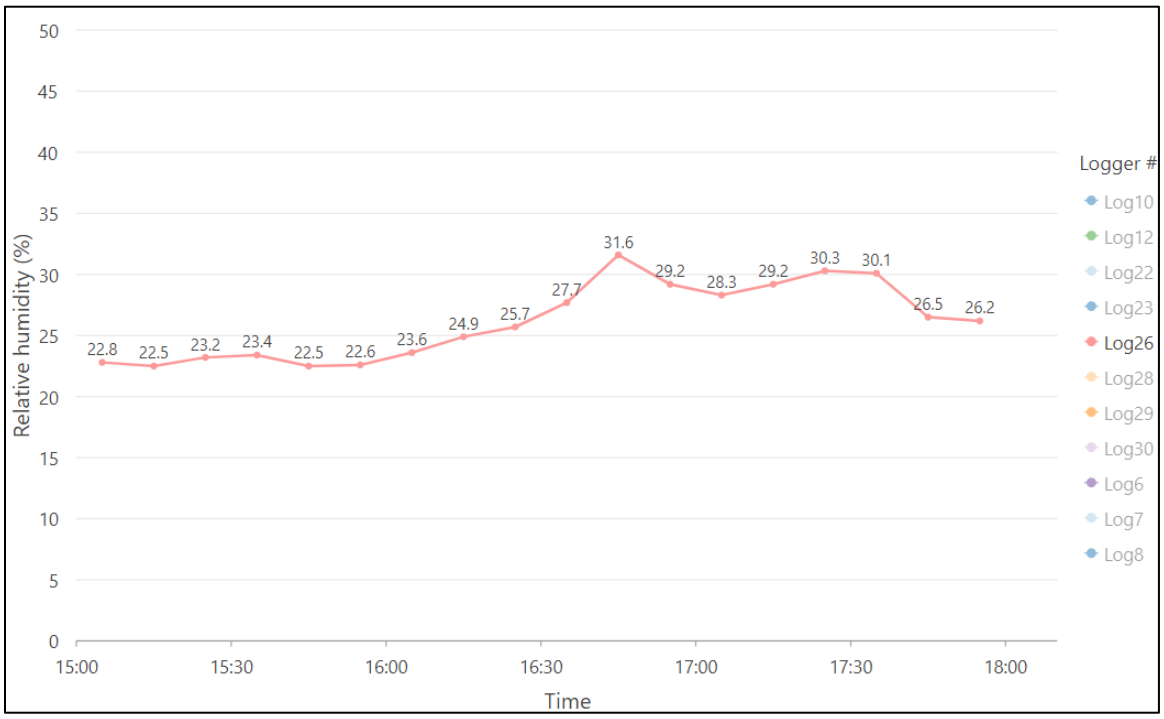

Figure 35: Downwind data logger 26 RH during the testing period using a 10 minute average of values.

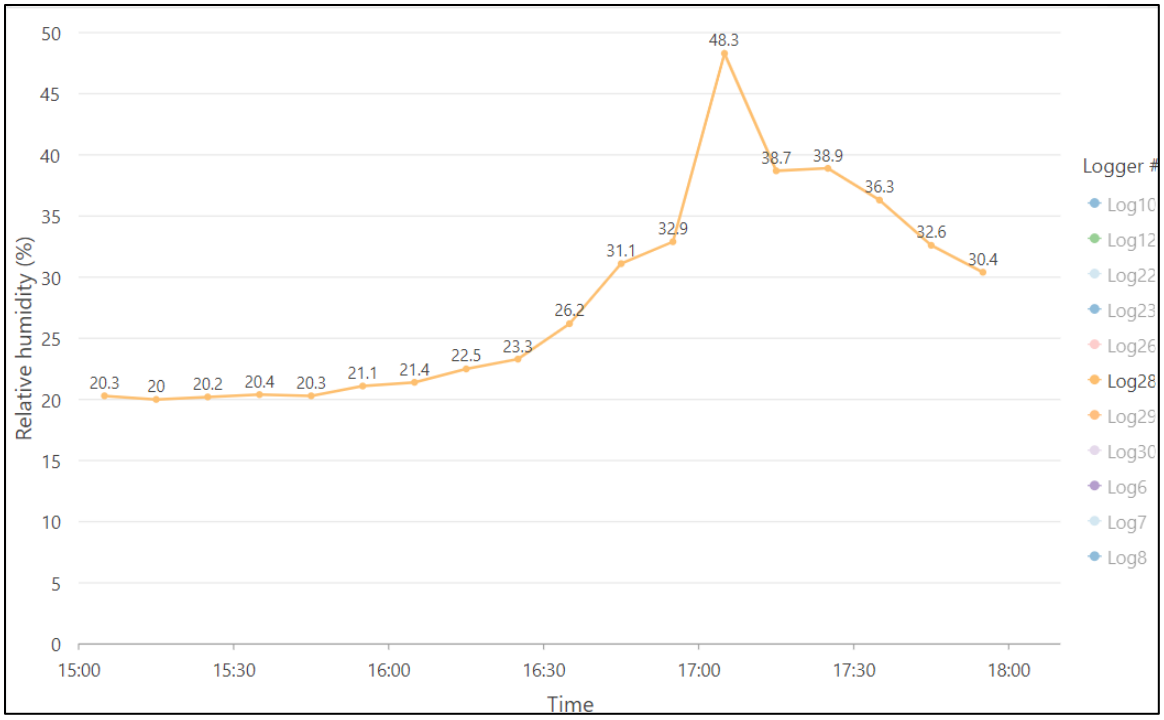

Figure 36: Downwind data logger 28 RH during the testing period using a 10 minute average of values.

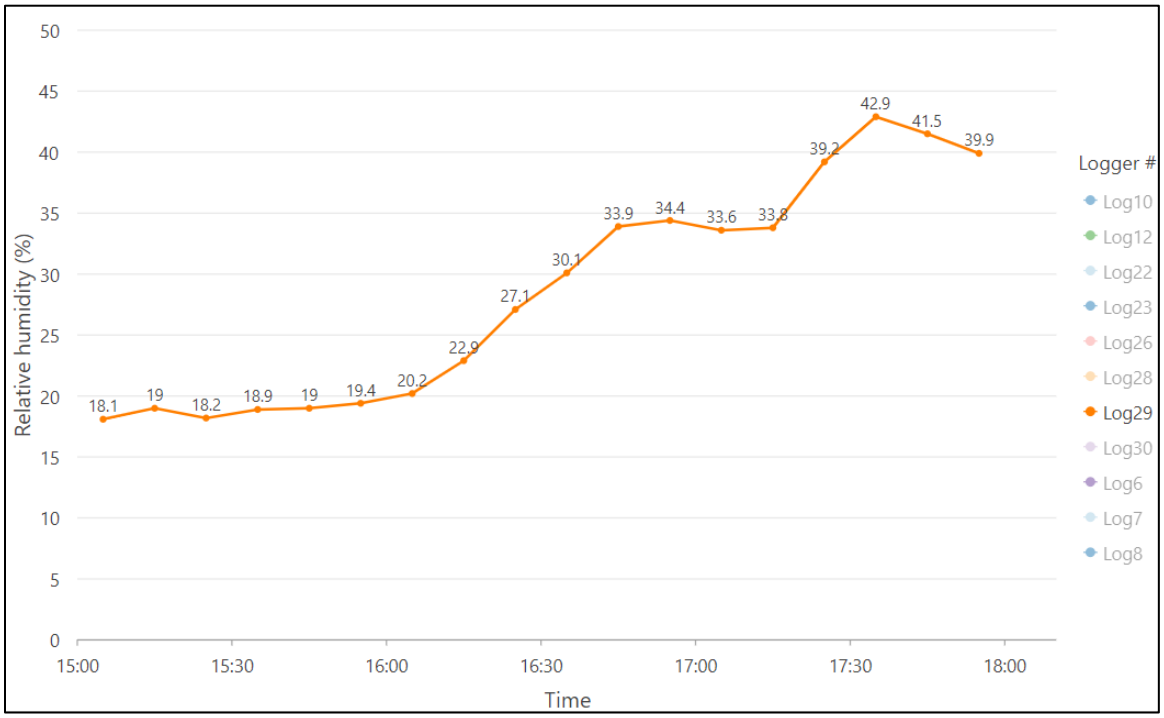

Figure 37: Downwind data logger 29 RH during the testing period using a 10 minute average of values.

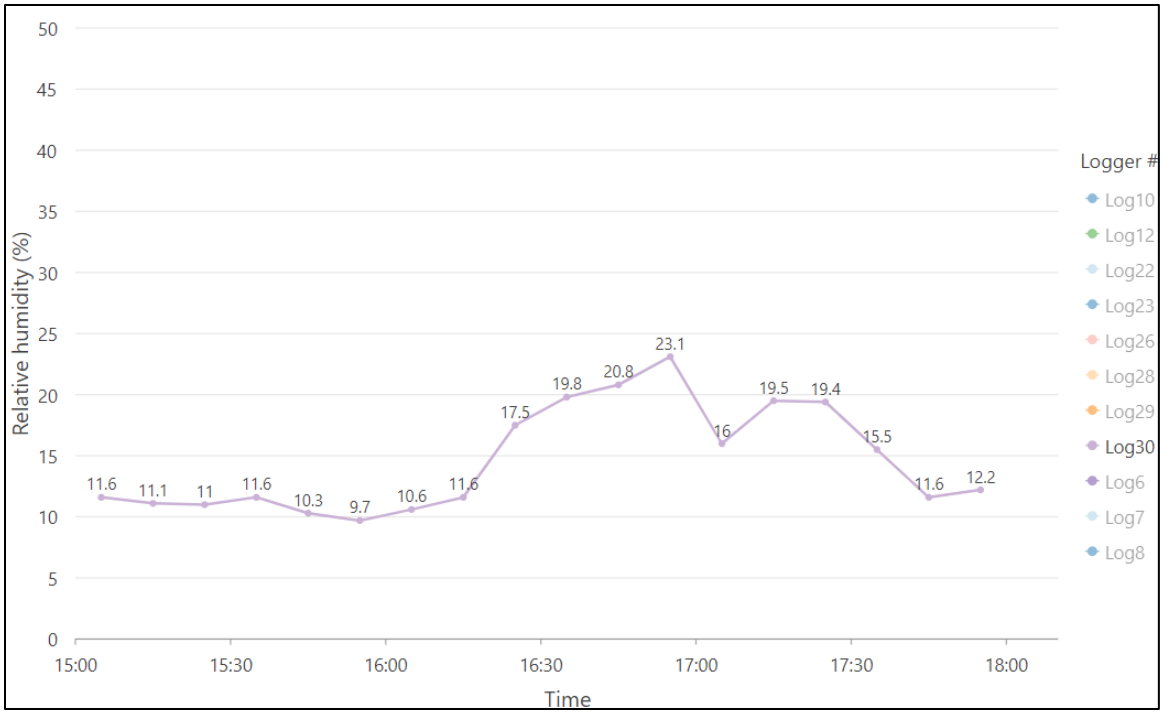

Figure 38: Downwind data logger 30 RH during the testing period using a 10 minute average of values.

Table 4: RH analysis using the ten minute average values that can be seen in Figures 19-38 for downwind data loggers.

Downwind data loggers	Pre-test RH average from 15:00 to 16:20 (%)	Test RH average from 16:20 to 17:30 (%)	Test RH average from 16:50 to 17:20 (%)	Largest increase from pre-test values (%)	Test RH 16:20 to 17:30 – pre-test average RH (%)	Test RH 16:50 to 17:20 – pre-test RH (%)	Post-test RH (%)	Post RH – pre-test RH (%)
10	20.3	21.4	21.775	2.7	1.1	1.5	20.7	0.4
12	21.6	20.2	20.275	0.6	-1.4	-1.4	20.4	-1.2
22	18.9	20.0	20.775	3.0	1.2	1.9	19.2	0.3
23	16.1	18.7	19.875	5.5	2.5	3.8	17.2	1.1
26	22.9	28.4	29.575	8.7	5.4	6.6	27.6	4.7
28	20.5	32.7	37.75	27.8	12.2	17.2	33.1	12.6
29	19.0	30.8	33.925	15.4	11.9	15.0	OUTLIER	
30	10.8	18.5	19.85	12.3	7.6	9.0	13.1	2.3
6	20.5	27.1	28.525	11.0	6.6	8.1	22.7	2.2
7	20.9	24.9	25.5	6.8	4.0	4.6	24.2	3.3
8	21.3	24.1	24.825	5.5	2.8	3.5	22.8	1.5
Max	22.9	32.7	37.8	27.8	12.2	17.2	33.1	12.6
Min	10.8	18.5	19.9	0.6	-1.4	-1.4	13.1	-1.2
Average	19.4	24.3	25.7	9.0	4.9	6.3	22.1	2.7

Table 5: RH analysis using the ten minute average values that can be seen in Figures 19-38 for upwind data loggers.

Upwind data loggers	Pre-test RH average from 15:00 to 16:20 (%)	Test RH average from 16:20 to 17:30 (%)	Test RH average from 16:50 to 17:20 (%)	Largest increase from pre-test values (%)	Test RH 16:20 to 17:30 – pre-test average RH (%)	Test RH 16:50 to 17:20 – pre-test RH (%)	Post-test RH (%)	Post RH – pre-test RH (%)
11	12.2	12.3	12.825	3.3	0.1	0.6	14.6	2.3
14	11.7	13.2	13.525	2.6	1.5	1.8	15.3	3.6
16	7.0	7.6	9	4.0	0.6	2.0	6.9	-0.1
18	12.6	17.4	18.8	6.8	4.8	6.2	20.1	7.5
19	5.2	10.5	11.9	7.6	5.3	6.7	13.7	8.5
24	12.6	13.7	14.875	3.6	1.1	2.2	13.3	0.7
25	9.4	11.3	12.025	3.5	1.8	2.6	11.7	2.2
13	OUTLIER							
9	OUTLIER							
Max	12.6	17.4	18.8	7.6	5.3	6.7	20.1	8.5
Min	5.2	7.6	9.0	2.6	0.1	0.6	6.9	-0.1
Average	10.1	12.3	13.3	4.5	2.2	3.2	13.6	3.5
All max	22.9	32.7	37.8	27.8	12.2	17.2	33.1	12.6
All min	5.2	7.6	9.0	0.6	-1.4	-1.4	6.9	-1.2
All average	15.8	19.6	20.9	7.3	3.8	5.1	18.6	3.1

FPInnovations

info@fpinnovations.ca
www.fpinnovations.ca

Follow us

OUR OFFICES

Pointe-Claire
570 Saint-Jean Blvd.
Pointe-Claire, QC
Canada H9R 3J9
(514) 630-4100

Vancouver
2665 East Mall
Vancouver, BC
Canada V6T 1Z4
(604) 224-3221

Québec
1055 rue du P.E.P.S.
Québec, QC
Canada G1V 4C7
(418) 659-2647